

**DESIGN OF ACOUSTIC META-MATERIAL
SOUND ABSORBERS BY FINITE ELEMENT
METHOD**

**A Thesis Submitted to
the Graduate School of Engineering and Science of
İzmir Institute of Technology
in Partial Fulfillment of the Requirements for the Degree of**

MASTER OF SCIENCE

in Mechanical Engineering

**by
Kaya MANOĞLU**

**July 2016
İZMİR**

We approve the thesis of **Kaya MANOĞLU**

Examining Committee Members:

Assist. Prof. Dr. Onursal ÖNEN

Department of Mechanical Engineering, İzmir Institute of Technology

Assoc. Prof. Dr. H. Seçil ARTEM

Department of Mechanical Engineering, İzmir Institute of Technology

Assoc. Prof. Dr. Abdullah SEÇGİN

Department of Mechanical Engineering, Dokuz Eylül University

28 July 2016

Assist. Prof. Dr. Onursal ÖNEN

Supervisor, Department of Mechanical Engineering, İzmir Institute of Technology

Prof. Dr. Figen KOREL

Deputy Head of the Department of Mechanical Engineering

Prof. Dr. Bilge KARAÇALI

Dean of the Graduate School of Engineering and Sciences

Dedicated to;
Berke MANOĞLU

ACKNOWLEDGMENTS

I would like to express thanks to my advisor Assist. Prof. Dr. Onursal ÖNEN for his guidance, support, encouragement and motivation during my study.

I am also grateful to Dr. Ş. Cihangir ÖZCANLI for his support and motivation during my thesis.

Lastly but most importantly, I offer sincere thanks to my parents for their love, motivation and support during my study.

ABSTRACT

DESIGN OF ACOUSTIC META-MATERIAL SOUND ABSORBERS BY FINITE ELEMENT METHOD

Acoustic meta-materials are widely known with their extra-ordinary sound properties like transmission, absorption and orientation which are not available in natural materials. These features are provided by their repeating constructions and various configurations. Sound absorbers are used in a wide variety of applications such as sound treatment in buildings, vehicles, concert halls and any place noise control and/or desirable acoustic properties are required. Traditional sound absorbers are long-known to be inefficient in the low frequency ranges. In this study, to overcome the absorption problem in low frequencies, absorption characteristics of foam based porous structures are analyzed with the addition of locally resonant blocks. Elements embedded in the absorber material with various shapes and properties are investigated by finite elements method to improve sound absorption, especially in the low frequency range. The results showed that embedding air cavities enclosed by thin solid shells to the absorber improves sound absorption in the low frequencies without significant deterioration in the high frequencies.

ÖZET

AKUSTİK META-MALZEME SES YUTUCULARIN SONLU ELEMANLAR YÖNTEMİ İLE TASARIMI

Akustik meta-malzemeler, ses yutum, iletim ve yönelim gibi sıra dışı akustik özellikleri ile yaygın olarak bilinmektedir. Bu özellikler, çok çeşitli konfigürasyonlara sahip periyodik olarak tekrarlayan yapılar olmaları ile ortaya çıkmaktadır. Ses yutucu yapılar ise başta evlerdeki ve arabalardaki ses yalıtımı olmak üzere gürültü kontrolünün ve arzu edilen akustik özellikleri elde etmenin gerekli olduğu bir çok alanda yaygın olarak kullanılmaktadır. Geleneksel ses yutucu yapıların düşük frekans değerlerinde oldukça etkisiz kaldıkları bilinmektedir. Bu çalışmada, bahsi geçen problemi ortadan kaldırmak için, köpük içerikli ve poroziteye sahip ses yutucu malzemelerin içerisine lokal rezonansa sahip periyodik bloklar eklenerek elde edilen yapıların ses yutum özellikleri analiz edilmiştir. Farklı şekillerde ve değişik özelliklere sahip periyodik yapıların gömülü olduğu köpük temelli yapılar sonlu elemanlar yöntemi kullanılarak özellikle düşük frekans değerlerinde ses yutumunu iyileştirmek amacıyla incelenmiştir. Elde edilen sonuçlar köpük temelli malzemelerin içerisine içi hava dolu silindir yapıların periyodik olarak eklenmesinin düşük frekanslardaki ses yutum özelliklerini, yüksek frekans değerlerini çok fazla düşürmeden geliştirdiğini göstermektedir.

TABLE OF CONTENTS

LIST OF FIGURES	x
LIST OF TABLES.....	xiv
CHAPTER 1. INTRODUCTION	15
CHAPTER 2. LITERATURE SURVEY.....	17
2.1. Porous absorption	17
2.1.1. Absorption mechanisms.....	17
2.1.2. Material types	18
2.1.2.1. Mineral wool.....	18
2.1.2.2. Foams.....	19
2.1.2.3. Environmentally friendly materials	19
2.1.2.4. Coustone	21
2.1.3. Basic material properties	22
2.1.3.1. Flow resistivity	22
2.1.3.2. Porosity	25
2.1.4. Modeling porous absorber sound propagation.....	25
2.1.5. Normal incidence	26
2.1.6. Oblique incidence	26
2.2. Resonant absorbers	27
2.2.1. Mechanisms	28
2.2.2. Applications	29
2.2.2.1. Bass trap membrane absorber	29
2.2.2.2. Helmholtz absorption.....	30
2.3. Absorbers with Inclusions	32
2.3.1. Helmholtz resonator inclusions	32
2.3.2. Micro-perforated absorbers.....	36
2.4. Impedance Matching	38

2.5. Acoustic Meta-materials	39
2.5.1. History	41
2.5.2. Geometries	43
2.5.2.1. Individual elements and geometries of the structures.....	43
2.5.2.2. Materials	44
2.5.2.3. Applications	44
2.5.2.4. Performance	45
2.6. Meta-material Absorbers	46
CHAPTER 3. FINITE ELEMENT MODELING.....	49
3.1. Acoustic Impedance.....	49
3.2. Empirical Model for Porous Absorber	50
3.3. Standing Wave Ratio(SWR) Method	51
3.4. Transfer Matrix Method	52
3.5. Finite Element Model	57
3.5.1. Comsol Multiphysics 5.0	57
3.5.1.1. Acoustics module.....	57
3.5.1.2. Generating the model.....	58
3.5.1.3. Geometry	59
3.5.1.4. Material properties	60
3.5.1.5. Initial conditions	61
3.5.1.6. Boundary Conditions	61
3.5.1.7. Meshing	62
3.5.1.8. Study	63
3.5.1.9. Obtaining the absorption coefficients	63
CHAPTER 4. RESULTS AND DISCUSSION.....	65
4.1. Absorber without the Addition of Cylindrical Elements.....	65
4.2. Absorber with Cylindrical Holes	66
4.3. Absorber with Different Hole Sizes	68
4.4. Absorber with Cylindrical Elements Filled with Foam.....	69
4.5. Absorber with Hollow Cylindrical Elements	73

4.5.1. Applying different outer diameters	74
4.5.2. Applying different materials	76
4.5.3. Applying different airflow resistivity values	77
4.6. Applying Inter-connected Inclusions	79
4.6.1. Transverse inter-connections	79
4.6.2. Longitudinal inter-connections	80
4.7. Longitudinal Air Channels	83
CHAPTER 5. CONCLUSIONS	86
5.1. Summary and Conclusions	86
5.2. Future Work.....	87
REFERENCES	89
APPENDICES	
APPENDIX A. MATLAB CODE FOR EMPIRICAL SOLUTION OF POROUS LAYER.....	93
APPENDIX B. MATLAB CODE FOR ABSORPTION COEFFICIENTS.....	95

LIST OF FIGURES

<u>Figure</u>	<u>Page</u>
Figure 2.1 The difference between closed (top) and open (bottom) pore constructions [2].....	18
Figure 2.2 Absorption properties of granulated rubber 1 mm to 3 mm in size for different thicknesses [2].....	20
Figure 2.3 Random incidence absorption coefficient obtained from a bonded flint absorber [2].	21
Figure 2.4 Geometry for sound propagation through a finite layer of a rigid-backed porous absorber [2].	27
Figure 2.5. Schematic presentation for (a) membrane, and (b) Helmholtz absorbers [2].....	28
Figure 2.6 Schematic presentation of a Helmholtz resonator	30
Figure 2.7 An example Helmholtz absorber and an application on the walls and ceiling in the auditorium of The Times Center [2].	31
Figure 2.8 Effects of different hole sizes and cavities to the Helmholtz Resonator [2]..	31
Figure 2.9 Geometry of the model [9]	32
Figure 2.10 Influence of SR opening orientation to the resonance frequency [9].....	33
Figure 2.11 Comparison between experimental and numerical results for the absorption coefficient of melamine layer with one of the SR inclusions [9]	33
Figure 2.12 Schematic presentation of the cellular material [10].....	34
Figure 2.13 Experimental setup of different PUC orientations in the impedance tubes [10].	35
Figure 2.14 Comparison of numerical and analytical results in different setups [10]....	35
Figure 2.15 Some clear micro-perforated absorbers [2].	36
Figure 2.16 Typical absorption coefficients for these some micro-perforated absorbers [2].....	37
Figure 2.17 Impedance matching layer by the bones in middle ear part of human ear [13].	39

Figure 2.18 Cubical acoustic meta-material samples.	40
Figure 2.19 Illustration of local resonances and the scatterings seen in the pressure pattern of meta-material structure.	40
Figure 2.20 (a) Eusebio Sempere’s sculpture in Madrid, Spain, (b) Measured sound attenuation as a function of frequency[21].	41
Figure 2.21 Cross section of a coated lead sphere and the illustration of 8x8x8 cubical structure [22].	42
Figure 2.22 Calculated (solid line) and measured (circles) amplitude transmission coefficient along the [100] direction as a function of frequency on the left, and calculated band structure of a simple cubic structure of coated spheres on the right [22].	42
Figure 2.23 Examples for the other shapes of acoustic meta-material elements.	43
Figure 2.24 Illustration of a three phase meta-material structure.	44
Figure 2.25 World’s first 3-D acoustic cloaking device hides objects from sound.	45
Figure 2.26 Different sound absorption properties in different directions [44].	47
Figure 2.27 Transmission spectrum of a single circular cell (red curve) with an attached mass of 0.11 g, and Sample-1 (blue curve) with an attached mass of 0.71 g. The left hand inset shows the front view of a planar array of square unit cells. The right hand inset shows the front view of a single circular cell [48].	47
Figure 2.28 The STL spectra of two nominally identical single-layer samples (red and green curves), together with the STL spectrum measured from the stacking of the two samples (blue curve). The purple curve is the STL spectrum of a broadband shield consisting of four single-layer panels [48].	48
Figure 3.1 Illustration of minimum and maximum pressure values.	51
Figure 3.2 Example of the minimum length of the pressure profile that must be taken to obtain SWR.	52
Figure 3.3 Schematic diagram of an experimental impedance tube setup.	56
Figure 3.4 Schematic illustration of the setup[49].	58
Figure 3.5 (A) Absorption coefficients obtained by finite element method and theory, (B) Absorption coefficients obtained by Oliva D. and Hongisto V., 2013 [49].	59

Figure 3.6 Comparison of the absorption coefficients obtained by 2D and 3D models..	60
Figure 3.7 Default boundary conditions of the models	61
Figure 3.8 Mesh types used in the models.....	62
Figure 4.1 Pressure diagram of the model at 2500 Hz without any inclusions.	65
Figure 4.2 Absorption coefficients of the porous media.	66
Figure 4.3 Schematic representation of the holes.	67
Figure 4.4 Acoustic pressure map of the structure for the frequency value of 3150 Hz.	67
Figure 4.5 Effect of holes to the absorption properties (r is the hole radius).	68
Figure 4.6 Absorption coefficients of two different setups	69
Figure 4.7 Schematic illustration of the model with the pipe thickness of 2mm.	70
Figure 4.8 Pressure diagram of the foam filled cylinder added model for the frequency of 3150 Hz.....	70
Figure 4.9 Absorption coefficients for the foam filled inclusions with different thickness values.	71
Figure 4.10 Absorption coefficients obtained from different inclusion material types for absorber with the pipe thickness of 1mm and outer hole diameter of 1 cm.	72
Figure 4.11 Pressure diagram of the air filled pipe embedded absorber for the frequency of 3150 Hz.....	73
Figure 4.12 Absorption coefficients for the air filled inclusions with the outer diameter of 1 cm with different thickness values.	74
Figure 4.13 Applied outer radiuses, (A) 2mm, (B) 3mm, (C) 4mm, (D) 5mm.	75
Figure 4.14 Absorption coefficients for different outer diameters, with constant thicknesses - $t = 0.2$ mm.	75
Figure 4.15 Absorption coefficients of the structures with different inclusion materials.	76
Figure 4.16 Absorption coefficients for different airflow resistivity values.	77
Figure 4.17 Pressure diagram of the square cross-section elements ($t = 2$ mm) including absorber.....	78
Figure 4.18 Obtained absorption coefficients for the square cross-section blocks.	78
Figure 4.19 Pressure diagram of the transverse inter-connected inclusions added absorber.....	79

Figure 4.20 The obtained absorption coefficients for the transverse inter-connections including elements added structure.....	80
Figure 4.21 Pressure diagram of the longitudinally interconnected inclusions added absorber.....	81
Figure 4.22 Absorption coefficients of longitudinally inter-connected inclusions added absorber	81
Figure 4.23 Corresponding pressure diagram for 3150 Hz	82
Figure 4.24 The absorption coefficients of the longitudinal inter-connections added elements including absorber	82
Figure 4.25 Comparison of different inter-connection types.....	83
Figure 4.26 The pressure diagram of the generated structure with the thickness value of 1.5 mm in 3150 Hz.	84
Figure 4.27 The absorption coefficients with different channel thicknesses.....	84

LIST OF TABLES

<u>Table</u>	<u>Page</u>
Table 2.1 Various empirical relationships for flow resistivity [2].....	23
Table 3.1 Delany and Bazley Coefficients[49].....	60
Table 3.2 1/3 Octave Band Frequencies.	64
Table 4.1 Hole diameter variations.....	67
Table 4.2 Sound velocity and density values of the used materials.	72

CHAPTER 1

INTRODUCTION

Acoustic absorption is the process of a material, structure, or an object absorbing, or taking in energy of the through-propagating sound wave. As an acoustic wave propagates through the material, some portion of the energy is absorbed and then transformed or dissipated into heat and remaining is transmitted through the absorbing body. The amount of this absorption differs from material to material, according to their physical properties. In general, soft, pliable, or porous materials such as sponge, foam and mineral wool show good acoustic absorbing properties, especially in the higher frequency range, on the other hand dense, stiff, impenetrable materials such as metals transmit the most of the energy without significant loss. As expected, while designing acoustic effective sound absorbers, choosing the right material is crucial in addition to geometric arrangement of the structure. In real life, sound absorbers are used in a wide variety of applications such as sound insulation and treatment in houses, nearly in all vehicles, aircrafts, concert halls and any place that requires noise control and desirable acoustic properties.

In this study, absorption characteristics of foam based structures are analyzed with the addition of locally resonant elements. Blocks with various shapes are investigated, which are embedded in the porous absorber material to improve sound absorbing properties, especially in the low frequency range, as porous materials are not efficient in this range. A parametric and a finite element study is performed to show the effects various design parameters to the absorbing properties, to develop an absorber effective in the low frequency range (up to ~ 300 Hz). Porous material is modeled by empirical Delany and Bazley coefficients and with the thickness of 5 cm. This thickness is held constant for all the models, but the physical and the geometric properties of the inclusions are varied to improve the low frequency problem. At first, foam is modeled without any inclusion, afterwards, secondly, bare air cavities are formed inside the foam to see the effect without any inclusions. Cylindrical inclusions are first generated as

simple shells filled with foam and different thicknesses. Shell material is specified as aluminum for all the models at first, to see the effect of the thickness variation. Then shell material is changed and several other materials including steel, lead, glass and spruce are tested. After that, the inner part of the shells which was filled with foam before are tested with filling removed (air cavity) and again different thicknesses and materials are tested. In addition to those parametric changes, also the effect of the airflow resistivity of the foam is varied (for representing different types of foam). Also, instead of using cylindrical blocks, elements with square cross-sections and model with both cylindrical and square cross-section profile are investigated.

The study is mainly based on finite element method in addition to some empirical models for porous materials. In the finite element solutions, Comsol Multiphysics is used. Comsol Multiphysics is a commercial finite element software used for solving the wide variety of engineering problems. All models are generated by using the Acoustics Module of the software and by applying the required conditions, solutions are investigated in 1/3 Octave band frequencies, between 100 Hz – 3150 Hz. Pressure diagrams and the absorption coefficients of all the models are shown and the results are discussed in the following sections. The results showed that the addition of the rightly chosen locally resonant blocks to a porous absorber improves the absorption characteristics of the structure in low frequencies. These additions enable having adequate low frequency absorption, which typically requires thick blocks of absorbers, without deterioration in higher frequencies. The results showed that using foam filled pipes makes the absorption even worse; while air filled ones improve the absorption properties for the low frequency band. Also, shell thickness came out to be a very important factor as less pipe thickness ends up in higher absorption coefficients.

CHAPTER 2

LITERATURE SURVEY

In this chapter, the literature survey on the topic including the main elements, parameters and absorption mechanisms is presented.

2.1. Porous Absorption

For better understanding the basics of porous sound absorption, it is required to understand the mechanism, effective parameters and material types which are commonly used for producing these kinds of absorbers. Porous absorbers are characterized by materials that contain many small diameter fibers or strands, often bonded to each other to lend some structural integrity. The most common types of porous absorbers are known as carpets, acoustic tiles, acoustic foams, curtains, cushions, cotton and mineral wool. These materials make sound propagate in the pores that are in connection and letting acoustic energy to be dissipated due to the viscous and thermal effects.

2.1.1. Absorption Mechanisms

In the simplest form, the mechanism for the porous absorption is based on the energy loss due to the propagation of sound through the material, in which isolated or interconnected pores present [1]. One of the main absorbing mechanisms is the viscous boundary layer effects. Air is a viscous fluid, and in a porous absorber, the sound energy dissipated due to the friction within the pore walls. In addition to the friction, some losses as a result of thermal conduction are present as well. For effective

absorption characteristics, there should be interconnected air channels through the surface and thickness of the material, to make the pores surface-open. A schematic showing the difference between the constructions of open and closed pore system is shown in Figure 2.1.

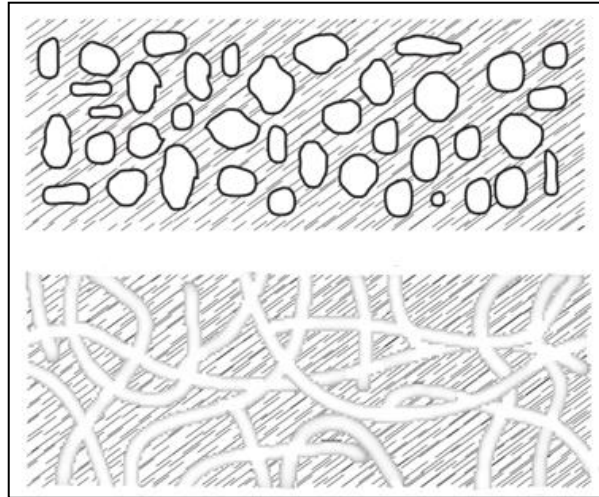


Figure 2.1 The difference between closed (top) and open (bottom) pore constructions [2].

In Fibrous materials like mineral wool, sound waves force the fibers to bend, and the generation of this bending results with the conversion of the acoustic energy to heat. This fibrous absorption mechanism is slightly different that the porous absorption since both of them are based on energy conversion.

2.1.2. Material Types

2.1.2.1. Mineral Wool

Mineral wools are usually made from sand, basaltic rock, recycled glass and similar materials. The raw materials are melted at high temperatures and then spun or pulled into wooly filaments. These fibers are then combined to form the shape of the product. Glass fiber is made from the same raw materials as normal glasses which are

sand, limestone, soda ash, etc. The acoustic absorption properties are relevant to the fiber composition, orientation, dimensions, product density and the quantity of the binder used [2].

The acoustic efficiency of the mineral wool materials depends on density, which can be explained as low-density products are not efficient for the high-frequency sound absorption. Man-made mineral wools are relatively low cost and they can be partially recycled. An important concern with man-made vitreous fibers are known to cause some long-term health effects such as breathing problems, skin irritation and others. The aforementioned problems can be solved by non-vitreous and fibreless absorbers, which are also discussed in the forthcoming sections.

2.1.2.2. Foams

Acoustic foam is a lightweight material made of polyurethane, polyether or polyester which are suited to be placed on the walls of a recording studio or a similar type of environment to act as a sound absorber, enhancing the sound quality within a room [3]. There are two types of foams in terms of pores, which can be said as open cell and closed cell structures. As expected, interconnected cell structure containing foams are tended to be more absorbent than closed cells due to their geometric properties which do not allow sound transmission into the material. Also, fire rating of these type of materials is important and classes of materials are available for different fire protection codes.

2.1.2.3. Environmentally Friendly Materials

These types of materials are mostly used as sound absorbers because they are environment-friendly, natural, renewable and plentiful. In this manner, instead of a mineral wool, suggestion of sheep wool has been made due to its less harmful effects to

the global warming [2]. Despite the fact that they are easy to manufacture, their low density results in thick material usage necessity in sound insulation applications.

The interest in the development of making acoustic absorbers from recycled materials is, also quite popular, motivating researchers and companies to develop sound absorbers from recycled materials such as clothes, metals, foams, various types wood, plastics or rubber. One typical example is the usage of acoustic properties of recycled tires as acoustic absorbers [2]. Another example is a study by Swift and Horoshenkov, who have shown that loose granulated mixes of waste foam with particle sizes smaller than 5 mm can be pressed into elastic, porous media with a high percentage by volume of open and interconnected pores, which provide very good absorption properties [4]. In another study, Pfretzschner tested rubber granular diameters ranging from 1.4 mm to 7 mm. Their findings of the typical absorption coefficients are presented in Figure 2.2. These results demonstrate that, for some frequency values, even the thinner absorbers might have higher absorption coefficients.[5].

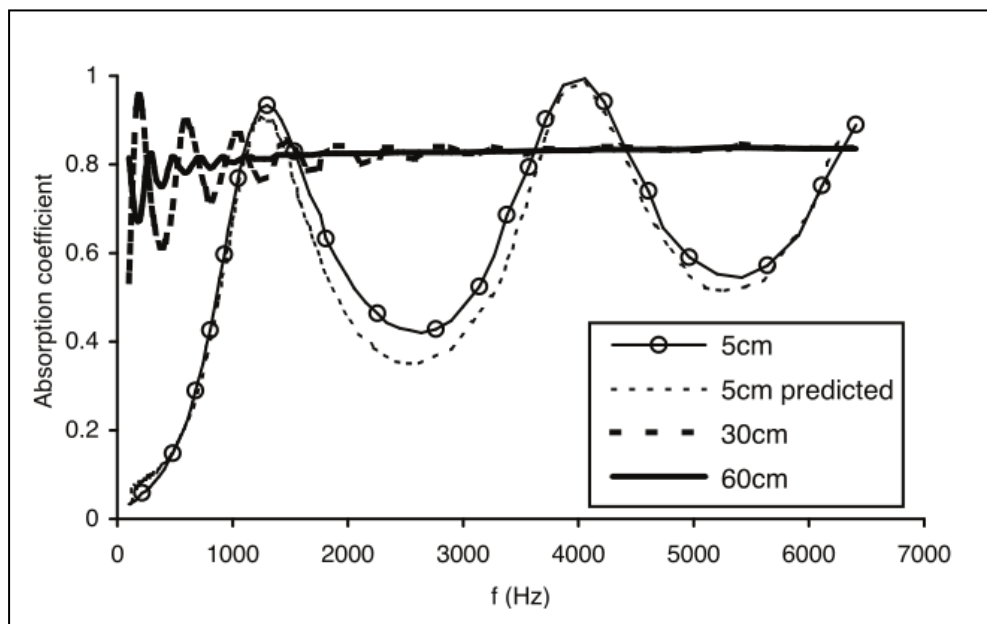


Figure 2.2 Absorption properties of granulated rubber 1 mm to 3 mm in size for different thicknesses [2].

2.1.2.4. Coustone

Coustone is a rigid, hard wearing material with a granulated facet which is built by bonded flint to keep the structure open and allow absorption. In addition to the absorbing properties, being washable is a very important fact which coustone provides. Leading to have a wide range of applications such as swimming centers, police interview rooms and firing ranges and etc. It provides a quite efficient sound insulation; since it is constructed from bonded flint, it is heavy, which is the main reason of high cost in the market. The material is shaped by combining the bonded flint with a resin. In Figure 3 typical absorption coefficients are shown under different conditions. It acts like a porous absorber, which has a little gap between the wall and the absorber, providing some extra absorption by moving it away from the low particle velocity region. In addition, it can also be supported by mineral wool to decrease cost and weight with the upcoming fringe benefits of better absorbing properties [2].

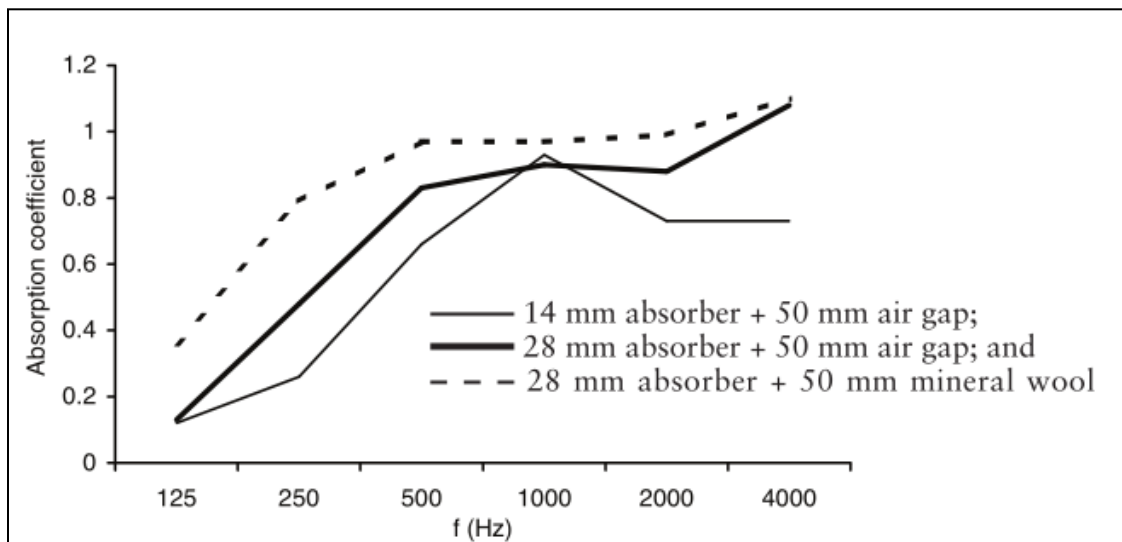


Figure 2.3 Random incidence absorption coefficient obtained from a bonded flint absorber [2].

2.1.3. Basic Material Properties

In this section of the study, mathematical modeling of porous absorbents of a typical porous material is explained in terms of the surface impedance and absorption estimation methods. These mathematical models also give an idea about how absorption is obtained and allows optimal design solutions for a specific absorption need. Two fundamental quantities which determine the sound absorbing behavior of sound within porous absorbents are discussed as first: Flow resistivity and porosity.

2.1.3.1. Flow Resistivity

Flow resistivity is the measure of resistance when air flow passes through the structure [2]. This is the way how the amount of sound energy loss within the material is obtained. For the formulation, a slice of the porous material with thickness d is considered. With the assumption of mean steady flow velocity U (U is a small value), the pressure drop ΔP is measured. From these two quantities, the flow resistivity σ ($Rayl/m$) is defined as:

$$\sigma = \frac{\Delta P}{Ud} \quad (2.1)$$

The flow resistance σ_s ($Rayl$) is defined as:

$$\sigma_s = \frac{\Delta P}{U} = \sigma d \quad (2.2)$$

The flow resistivity corresponds to the resistance per unit material thickness. Therefore, if the flow velocity is high, this means non-linear factors should be taken into consideration [2]. The flow resistivity formulations written below are not valid for high-pressure sound waves, approximately when sound pressure levels are higher than 140 dB [2]. The unit of flow resistance in MKS unit system is $Nm^{-3}s$, or one Rayl. Flow resistivity is one of the most important to absorption properties of a porous absorber.

Table 2.1 Various empirical relationships for flow resistivity [2].

Material	Formulation
Parallel to the fibres, all fibres having the same radii	$\sigma = \frac{3.94\eta(1 - \varepsilon)^{1.413}[1 + 27(1 - \varepsilon)^3]}{a^2\varepsilon}$
Perpendicular to the fibres, all fibres having the same radii	$\sigma = \frac{10.56\eta(1 - \varepsilon)^{1.531}}{a^2\varepsilon^3} \quad 6 \leq a \leq 10\mu\text{m}$
	$\sigma = \frac{6.8\eta(1 - \varepsilon)^{1.296}}{a^2\varepsilon^3} \quad 20 \leq a \leq 30\mu\text{m}$
Random fibre orientation, all fibres having the same radii	$\sigma = \frac{4\eta}{a^2} \left[\frac{0.55(1 - \varepsilon)^{4/3}}{\varepsilon} + \frac{\sqrt{2}(1 - \varepsilon)^2}{\varepsilon^3} \right]$
Random fibre radius distribution with a mean radius of a , and random fibre orientation.	$\sigma = \frac{3.2\eta(1 - \varepsilon)^{1.42}}{a^2} \quad \text{fibreglass}$
	$\sigma = \frac{4.4\eta(1 - \varepsilon)^{1.59}}{a^2} \quad \text{mineral fibre}$
Polyester fibreous materials $18 \leq 2a \leq 48 \mu\text{m}$ $12 \leq \rho_m \leq 60 \text{ kgm}^{-3}$ $900 \leq \sigma \leq 8500 \text{ rayls m}^{-1}$	$\sigma = \frac{25.989 \times 10^{-9} \rho_m^{1.404}}{(2a)^2}$
Polyester fibre $6 \leq 2a \leq 39 \mu\text{m}$ $28 \leq \rho_m \leq 101 \text{ kgm}^{-3}$ $900 \leq \sigma \leq 8500 \text{ rayls m}^{-1}$	$\sigma = \frac{15 \times 10^{-9} \rho_m^{1.53}}{(2a)^2}$
Sheep wool $22 \leq 2a \leq 35 \mu\text{m}$ $13 \leq \rho_m \leq 90 \text{ kgm}^{-3}$	$\sigma = \frac{490 \times 10^{-6} \rho_m^{1.61}}{2a}$
Wood materials with short fibres $2a \approx 30 \mu\text{m}$	$\sigma = 20.8 \rho_m^{1.57}$
Loose granular materials	$\sigma = \frac{400(1 - H^2)(1 + H^5)\mu}{HD}$ $H = 1 - \rho_m / \rho_f$
Consolidated granular material	$\log_{10}(\sigma) = -1.83 \log_{10}(D) - 0.96$

Notes: η is the viscosity of air (1.84×10^{-5} poiseuille) and ε the porosity; $\varepsilon = \rho_m / \rho_f$ where ρ_f is the density of the fibres or the grain material and ρ_m the bulk density of the material. D is the characteristic particle dimension: $D^2 = V_g / 0.5233$ where V_g is the number of the particles in a unit volume.

There are few formulations in the literature that can be used to determine the flow resistivity, like the one quoted below, derived by Bies and Hansen which corresponds to fiberglass [6].

$$\sigma = 7.95 \times 10^{-10} \left(\frac{\rho_m^{1.53}}{a^2} \right) \quad (2.3)$$

where a is the fiber radius and ρ_m is the bulk density of the absorber. Bies and Hansen showed that fibrous materials almost have a linear relationship between flow resistivity and density however this is not valid for foam [6].

There are several other empirical relationships have been reported which deal with various materials, such as granular materials, larger fiber sizes. If required, these relationships can be found in the literature (Table 2.1).

Formulations to estimate the effect of temperature on the properties of a porous absorber can be expressed similarly: A temperature increment increases the flow resistivity.

A basic formulation can be written as:

$$\sigma(T) = \sigma(20) \left(\frac{273+T}{293} \right)^{1.65} \quad (2.4)$$

where T is the temperature in °C and $\sigma(20)$ is the flow resistivity at 20°C [7]. When using this equation with the upcoming formulations for impedance, it is required to modify the sound velocity and gas density for the corresponding temperature:

$$c(T) = c(20) \left(\frac{273+T}{293} \right)^{1/2} \quad (2.5)$$

$$\rho(T) = \rho(20) \left(\frac{273+T}{293} \right) \quad (2.6)$$

For thin cover materials which are used to cover porous absorbers, it makes better sense to define properties in terms of the flow resistance. Because it is possible to fabricate and use materials like wires, glass fibers and clothes with a wide range of flow resistance values.

2.1.3.2. Porosity

Porosity can be explained as the provided air volume inside the absorbent. It is defined as the ratio of the total pore volume to the total volume of the absorbent. Mostly, good absorbers have high porosity values, for instance most mineral wool types have a porosity value about 0.98, but when designing an absorber, flow resistivity is preferable to porosity. In the estimation of porosity, closed pores are not included in the pore volume as they are inaccessible for the sound waves and for measurement tools.

2.1.4. Modeling Porous Absorber Sound Propagation

Modeling the propagation of sound within a porous absorbent is not very easy. There are basically two approaches which are found to be most useful. First one is a completely empirical approach, first presented by Delany and Bazley, which is based on measuring a large number of samples of porous materials and using curve fitting to obtain the relationship which describes the effect of characteristic impedance and the propagation wave number to the flow resistivity [8]. When applied to a simple material, this technique works quite well and is simple to use.

A second approach to modeling porous absorbent is formulating the problem using a semi-analytical approach. For example, modeling propagation within the pores is possible on a microscopic scale. However, this approach results in rather complicated theoretical models, of which there are only a few variants in the literature. Since it is known that in most porous absorbents, all the parameters within the model are not possible to be derived analytically, making this approach hard to apply. Particularly, factors relevant to the pore shapes are difficult to estimate except empirically. Nevertheless, this type of modeling is the best way of enabling the design and development of the next generation porous absorbers without a complete empirical approach.

2.1.5. Normal Incidence

The propagation direction within many porous absorbers is normal to the surface, and therefore it is much easier to evaluate. As known from the Snell's law, angles of propagation are relevant to the sound velocity in the material [2]. The wave number in air is k_0 , and the wave number in the material is k . In vector form, the wave number of air k_0 , and the wave number of the material k are written as $k_0 = \{k_{0,x}, k_{0,y}, k_{0,z}\}$, $k = \{k_x, k_y, k_z\}$ and $k_{0,y} = k_y = k_{0,z} = k_z = 0$. As it is known that $k^2 = k_x^2 + k_y^2 + k_z^2$, the wave number is written as $k = k_x$. This can be used to obtain an alternative formulation for surface impedance of a rigidly backed absorber for normal incident:

$$z_{sl} = -jz_c \cot(k_x d) \quad (2.7)$$

where z_c is the characteristic impedance of the absorbent.

2.1.6. Oblique Incidence

When sound waves hit the absorber material not perpendicularly but with an angle, this is called as an oblique incidence. Consider a sound wave in air incident on a finite layer of porous material with a rigid backing at an angle ψ shown in the Figure 2.4. As shown in the previous section, the wave number of air k_0 , and the wave number of the material k can be shown respectively in vector form as $k_0 = \{k_{0,x}, k_{0,y}, k_{0,z}\}$, $k = \{k_x, k_y, k_z\}$ and $k_{0,z} = k_z = 0$. In terms of wave number, this formulation can be written:

$$k_y = k_{0,y} = k_0 \sin(\psi) = k \sin(\beta) \quad (2.8)$$

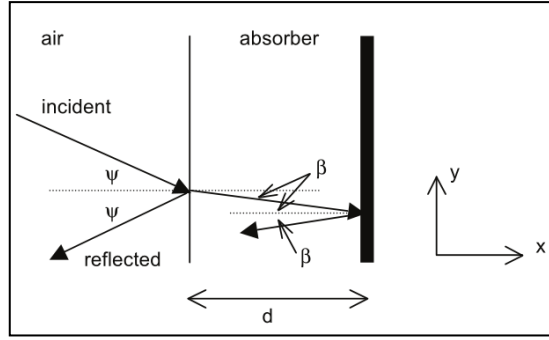


Figure 2.4 Geometry for sound propagation through a finite layer of a rigid-backed porous absorber [2].

The wave number in most of the porous absorbers, is very different from the wave number in air. The wave number in absorbent that $\beta \rightarrow 0$ and the previous derived normal incident formulation is quite accurate. However for the cases where $\beta > 0$, a different formulation can be derived. As $k^2 = k_x^2 + k_y^2 + k_z^2$, this can be combined with Equation 2.8 to obtain:

$$k_x = \sqrt{k^2 - k_y^2} \quad (2.9)$$

The square root with the positive real part must be chosen. This can be used to obtain alternative formulation for surface impedance of a rigidly backed absorber for oblique incident.

$$z_{sl} = -jz_c \frac{k}{k_x} \cot(k_x d) \quad (2.10)$$

where z_c is the characteristic impedance of the absorbent [2].

2.2. Resonant Absorbers

One of the best ways to solve the low frequency sound absorption problem is using the science behind the phenomenon of resonance. In the cases where sufficient absorption cannot be obtained, especially in low frequencies with porous absorbers. The material thickness should be at least $1/4^{\text{th}}$ of the wave length of interests leading to thick and expensive material cost. Due to the required material size and thickness for porous

absorbers, resonant absorbers are the proper solution to achieve the desired absorption coefficient. There are fundamentally two common types of these absorbers: First type is the Helmholtz absorber which is named after the German physician Hermann von Helmholtz and the second type is membrane absorbers-also known as panel absorbers. In the recent years, more improved devices have been produced based on the same logic and physics. Characteristics of Helmholtz resonators can be predicted reasonably accurate compared to membrane absorbers. All these resonant absorbers are essentially effective for low- frequency sound absorption, for example they are mostly used for low frequency room modes and as parts of silencers within ventilation systems.

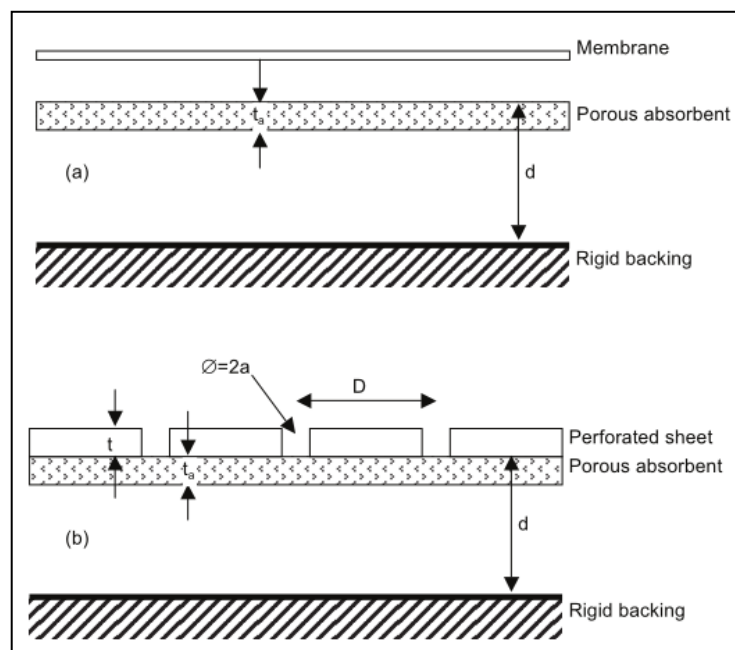


Figure 2.5. Schematic presentation for (a) membrane, and (b) Helmholtz absorbers [2].

2.2.1. Mechanisms

Resonant absorbers can be modeled as a mass-spring system. The two common types of resonant absorber are shown in Figure 2.5. Difference of a Helmholtz absorber is the mass which has a plug of air in the opening of the perforated sheet. The resonance is generated same way like blowing across a bottle. To apply this into an absorber, some damping must be provided to get rid of the sound energy; which is usually created by a

thin layer of mineral wool. For a membrane absorber, the mass is a sheet of material like rubber or mass added vinyl that vibrates. Adjusting the resonant frequency by changing the vibrating mass and the stiffness of the air spring is possible, which helps to achieve good absorption properties. Damping is a must for energy dissipation, usually provided by placing porous absorbent at the places, where the particle velocity is high. (For the Helmholtz resonator it is the neck of the absorber and for panel absorber just behind the membrane.) The important part is not placing the absorber too close to the membrane which prevents the movement of the membrane. Additionally, some types of Helmholtz resonators with small openings can provide energy dissipation without using porous absorbents. Actually this is a method to create resonant absorbers like micro-perforated absorbers without using porous absorbers. In the cases of panel absorbers, occurrence of internal losses within the vibrating membrane also exists however they are too small to generate high absorption.

2.2.2. Applications

In this section, two applications of resonant absorbers including bass trap membrane absorber and Helmholtz absorber are presented.

2.2.2.1. Bass Trap Membrane Absorber

Poor low frequency response is a very frequent problem for small rooms. The reason is modal excitation's being too small in addition to the limited space within, which makes it hard to place the treatments. Porous absorbers are not effective at those frequencies due to the particle velocity which is essentially zero near walls and in corners for long wavelengths. By using a resonant absorber like using a membrane design, it is possible to solve that problem, since it is known that a membrane absorber can be effective in absorbing high sound pressure fluctuations present at wall surfaces

and in the corners in the modal frequency range. Because of that reason, usage of sub-woofer absorbers became very popular in the last few years. The schematic presentation of the device is shown in Figure 2.5. Pressure fluctuations are transformed into air motion by the membrane. The more membrane vibrates over a selective low frequency, the more it pushes air through an internal porous layer that generates low frequency sound absorption.

2.2.2.2. Helmholtz Absorption

A Helmholtz resonator or Helmholtz oscillator can be described as a gas container with an open hole which is called as neck or port (Figure 2.6). A volume of gas (air) inside and near the open hole vibrates due to the elastic movement of the air inside the container. The most typical example is an empty bottle blown across from the top. The vibration or resonance of the air inside at a certain frequency can be heard or observed. This frequency is specific to the geometry and structure of Helmholtz resonator, is called as the resonance frequency.

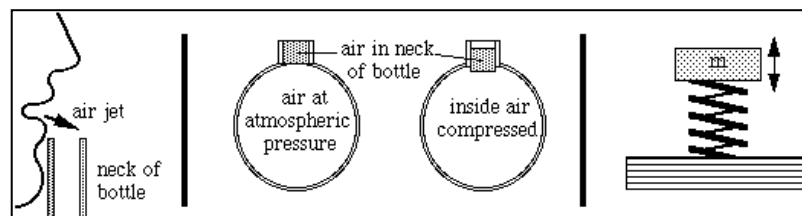


Figure 2.6 Schematic presentation of a Helmholtz resonator

Nowadays, wood is not only being used as a surface material but also as an absorbent material. However, one of the biggest problems caused by flat wooden panels is the generations of unwanted sound reflections which lead to difficulty in speech intelligibility and low music quality. To prevent those undesired reflections, fiberglass coverings are being applied. Furthermore, some wooden panels are being used to provide absorption at specified frequency ranges.



Figure 2.7 An example Helmholtz absorber and an application on the walls and ceiling in the auditorium of The Times Center [2].

The system and the example application is shown in Figure 2.7. Changing the geometric properties like groove spacing, hole diameter, and the rear air cavity depth and content allows obtaining absorptions at specific frequencies according to the purpose. Parametric effects to the absorption coefficients are presented in Figure 2.8.

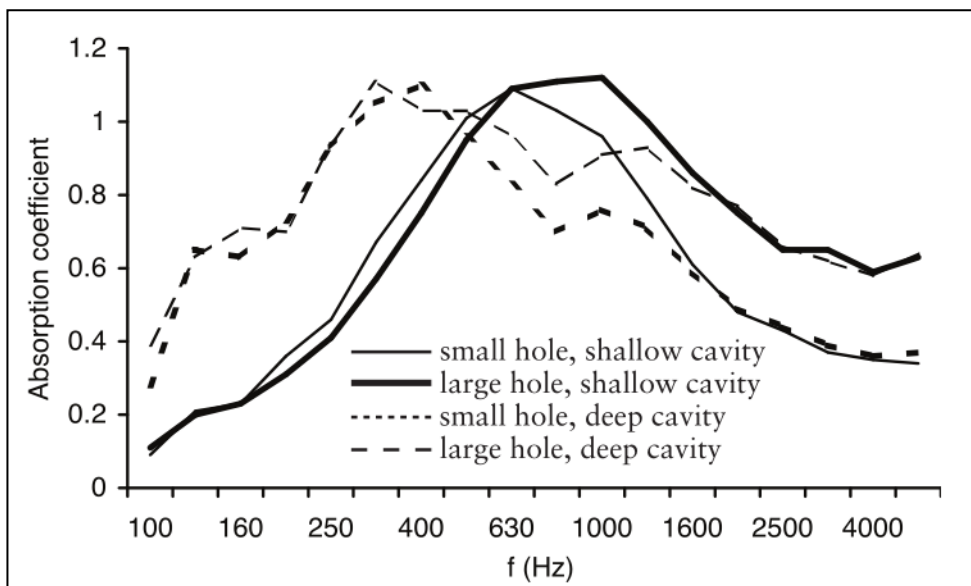


Figure 2.8. Effects of different hole sizes and cavities to the Helmholtz Resonator [2]

These Helmholtz absorbers are produced from medium density fiber board (MDF) and the backing is covered with a non-woven glass matt to generate resistance.

2.3. Absorbers with Inclusions

For sound absorption, porous materials are widely used in wide variety of applications. But, when these absorbers are applied with a rigid backing, they are only effective if their thickness is longer than a quarter of the sound wavelength [2]. This makes use of thicker layers mandatory if absorption of low frequency is required. A traditional method to overcome this problem is using multi-layered structures. Making it possible to use thinner layers, compared with the single layer porous absorbers, using embedded periodic set of resonant inclusions is another way to make absorbers more efficient without the need for thick, multi-layer assemblies.

2.3.1.1. Helmholtz Resonator Inclusions

An investigation for an alternative way for multi-layered structures by embedding a periodic set of resonant inclusions is recently studied [9]. In the study, resonant inclusions with a split ring (SR) shape cross section are used (Figure 2.9).

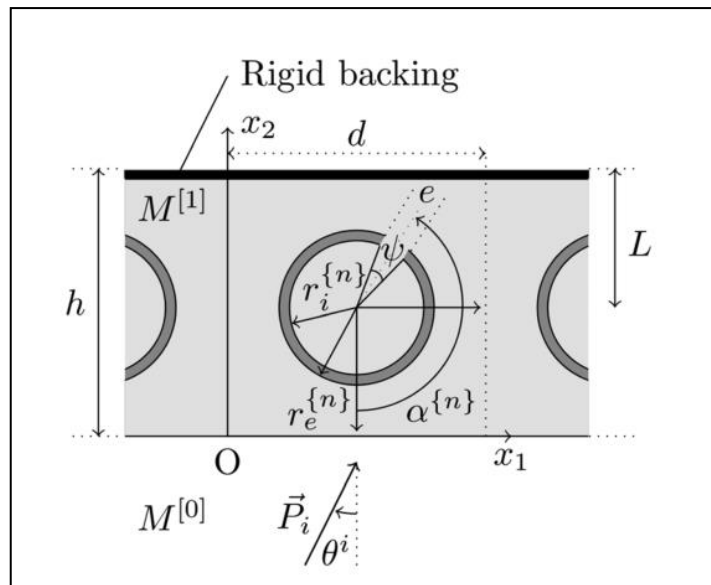


Figure 2.9 Geometry of the model [9].

The inclusions and the porous material that generates the absorber are considered as static. Each unit cell, includes SR in the center with the lattice constant of 2 cm. The porous material matrix is made out of Fire-flex (Recticel, Belgium) with a rigid plate backing. Fire-flex is a foam like fire resistant material that provides good acoustic performance. In the study, resonance frequencies with different SR orientations are obtained. (Figure 2.10).

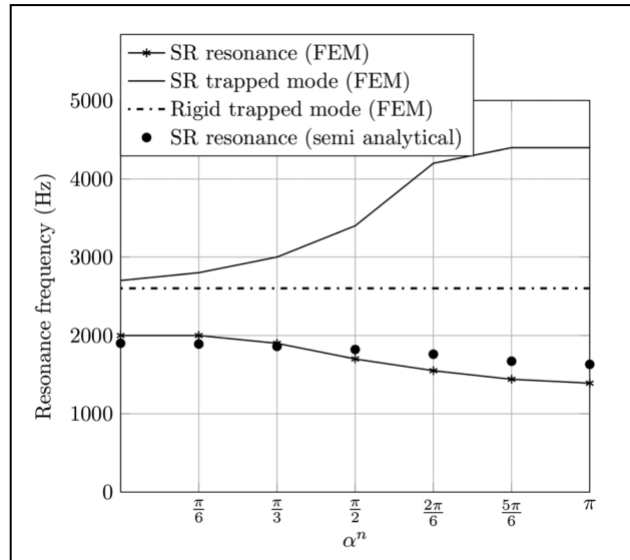


Figure 2.10 Influence of SR opening orientation to the resonance frequency [9].

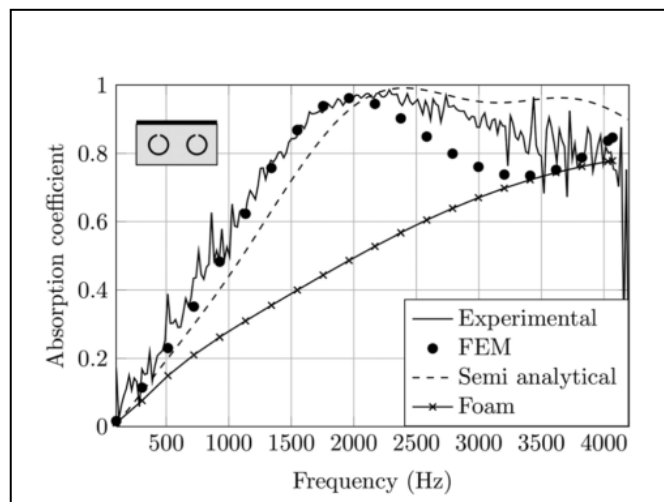


Figure 2.11 Comparison between experimental and numerical results for the absorption coefficient of melamine layer with one of the SR inclusions [9]

The study clearly shows that inclusions lead to an increase in the absorption coefficients for low frequency applications. The reason of the increase in the absorption coefficients is the excitation mode triggered by the periodic arrangement of the inclusions, which provides energy entrapment. Trapped mode provides better absorption properties for frequencies below the quarter-wave length resonance of the porous layer when the structure is placed against a rigid boundary (Figure 2.11).

And also higher absorption coefficients in lower frequencies are being possible due to the resonances of the inclusions. As a result, adding resonant inclusions in a porous layer absorber can be an alternative to multi-layered and double porosity materials in the design of sound absorbers for low frequency purposes. In another study, analytical and numerical modeling is supported with the experimental verification of large sized cellular resonant porous materials. They are combined with spherical Helmholtz resonator(HR) inclusions [10]. Periodic Unit Cell (PUC) is modeled as a combination of porous element to see the absorption properties as well as parallel element series to see absorption properties in terms of Helmholtz behavior(Figure 2.12). Main purpose of the study is the investigation of sound absorption and transmission loss with respect to the HR. Also experimental study is done by using an impedance tube to see the effect of the orientation to the sound absorption (Figure 2.13).

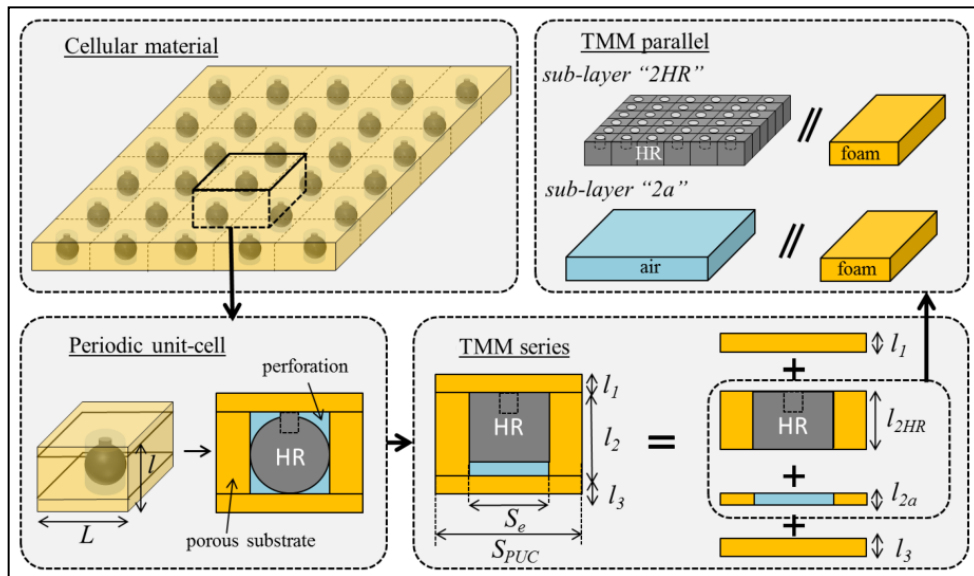


Figure 2.12 Schematic presentation of the cellular material [10].

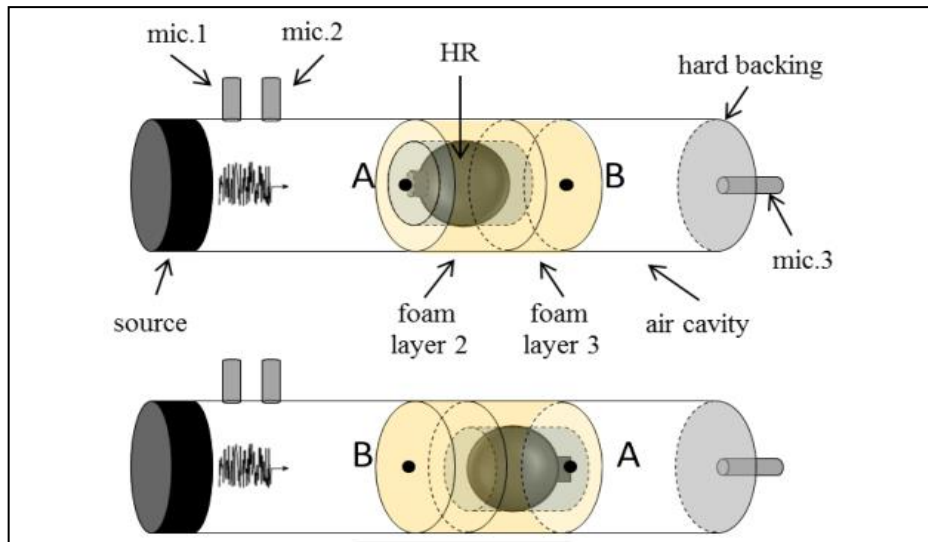


Figure 2.13 Experimental setup of different PUC orientations in the impedance tubes [10].

Experimental, analytical and numerical results are in excellent agreement and the study shows that the attenuation property of the material is greatly improved at the HR resonance frequency (Figure 2.14). It is also shown that, adding HR to the setup makes negative effect to the sound absorbing efficiency of the porous host material at the HR resonance frequency and this decrease is explained due to the neck orientation of the resonator.

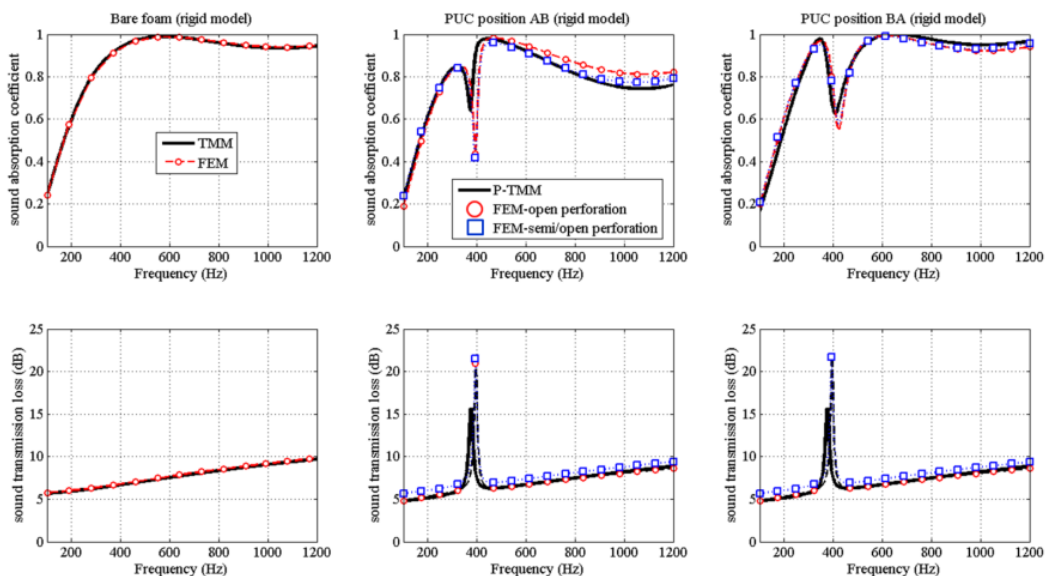


Figure 2.14 Comparison of numerical and analytical results in different setups [10].

2.3.2. Micro-perforated Absorbers

Production of fully transparent absorbers to control sound absorption in a room, while having a view through the glazing is an important fact which brings an option of tunable lighting properties for a room. A micro-perforated panel absorber is backed by an air-cavity with a rigid-back wall and it is typically used for absorbing sound. Glazing is a common building material, and provides saving on materials and cost by combining lighting and acoustic function into one device. These properties are achieved by applying micro-perforation to the materials like illustrated in Figure 2.15.

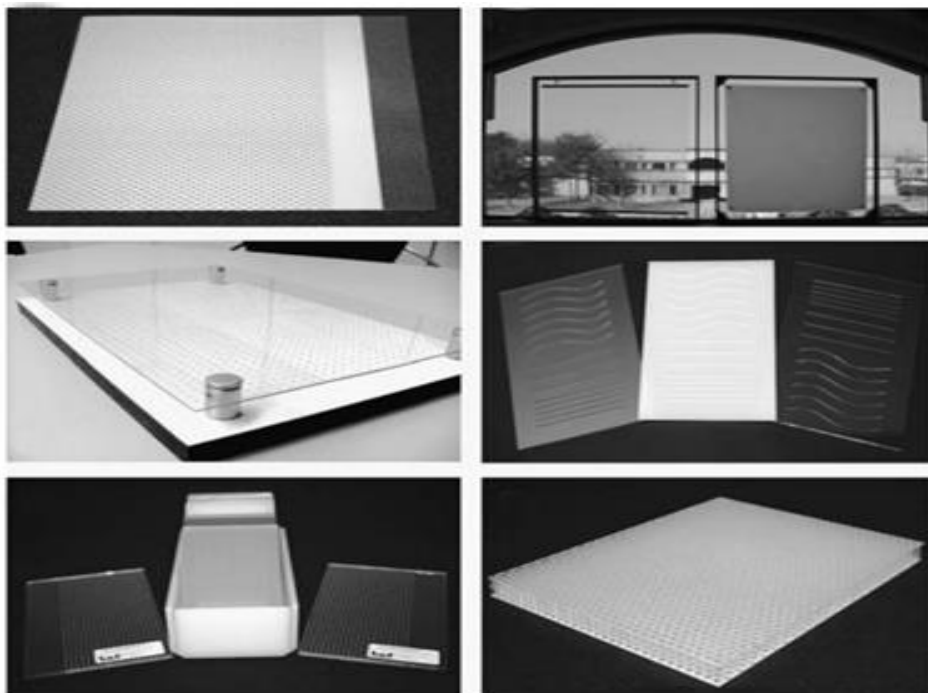


Figure 2.15 Some clear micro-perforated absorbers [2].

These absorbers are mostly used as Helmholtz devices without any resistive material. For example, the device might contain double glazing units, whose first panel has a thickness of 5 mm including sub-millimeter diameter holes spaced 5 mm apart. This device have good absorption properties provided by high viscous losses as air passes through the small holes, which are a little larger than the boundary layer.

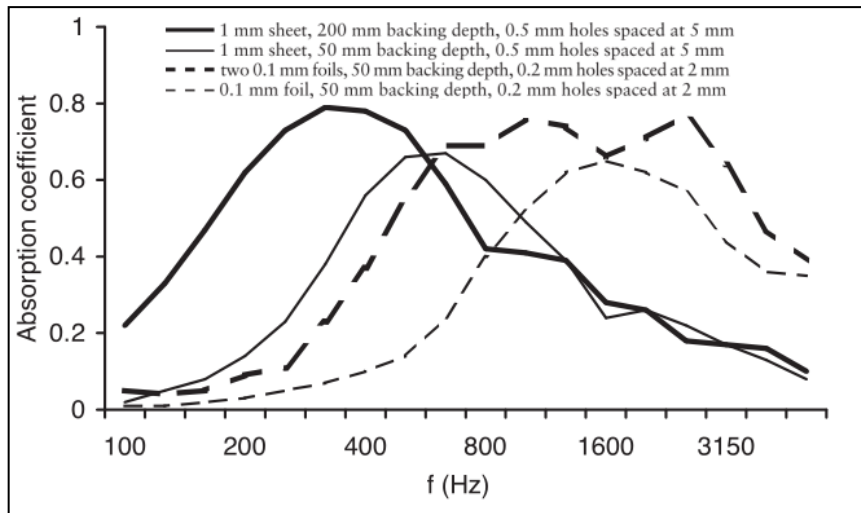


Figure 2.16 Typical absorption coefficients for these some micro-perforated absorbers [2].

This effective absorption in low frequencies eliminates the need for using porous materials in the air cavity between the perforated layer and the backing surface. For increasing low frequency absorption, geometry of the device can be changed by designing curved, tilted shapes. The surfaces are transparent from the perpendicular view, but at oblique angles the holes become more visible [2].

Helmholtz devices with the thicker sheet materials, the absorption is not as controllable as Helmholtz devices with resistant material. Thicker materials work well in low to mid-frequency against noise and reverberance problems in rooms like atria. In terms of thickness of the material, Maa studied the concepts of micro-perforation revealing that the frequency band of sound absorption of a perforated-panel construction depends essentially on the diameter of the perforations, and micro-perforated panels with sub-millimeter holes are providing good absorption characteristics [11].

The results show that using thinner materials are necessary for speech intelligibility aimed sound absorption. It is possible to say that the absorber, which has smaller holes in diameter, with the thickness of 0.1 mm has better absorption properties for the frequencies higher than 700 Hz. On the other hand, adding an air cavity to the perforated absorber with thickness of 1 mm and 0.5 mm holes gives higher absorption coefficients for the frequencies under 400 Hz. Figure 16 shows typical absorption coefficients for two different materials and layer thicknesses. The foil can be made out

of a material such as polycarbonate and double layering can be effective for widening the absorption range. An example showing the difference in one and two layers of micro-perforated foils are shown in Figure 2.16[2]. The biggest advantage of clear micro-perforated absorbers is that they can be hung some way from the backing surface without making the room darker or smaller. Also additional backing depth can improve the low frequency absorption performance. A double layer construction or extraporous absorbent is necessary if broader frequency range for absorption is required [2].

Micro-perforation is also preferable even when transparency is not necessary. By using right material, these absorbers can withstand worse environmental conditions compared with porous absorbers in harsh environments. The holes can be clogged up easily with dust or dirt but in the case where mechanical vibrations present, the holes are not frequently blocked, are also unexpectedly very hard to get clogged up even in very dusty environments because of the vibration of the pores due to the movement of the air plug inside. Additionally, double layered setups are widely used in aircrafts and cars where low weight is an important fact [2].

2.4. Impedance Matching

Impedance matching can basically be defined as providing the compliance of the impedance values of two different media in which sound waves are transmitted from one to another. This is actually a big problem if the acoustic impedance of two media are in a big contrast, which results in the majority of sound energy back to the incident media rather than being transferred to the other. For example, in medical ultrasonography, the gel is an impedance match agent, which is used to transfer acoustic energy from the transducer to the body and back. In the vicinity of the gel, the impedance contrast in the transducer-to-air and the air-to-body will nearly result in almost complete back reflection of the energy, without waves transferred to the body for imaging. The middle ear works as an impedance-matching device that makes sound transmission more efficient, reduces the amount of reflection and protects the inner ear from hazardous sound pressure levels. This protection is actively adjusted by the brain

using the middle ear's muscles to tense and un-tense the bone structure with a reaction speed as fast as 10 milliseconds [12]. (Figure 2.17).

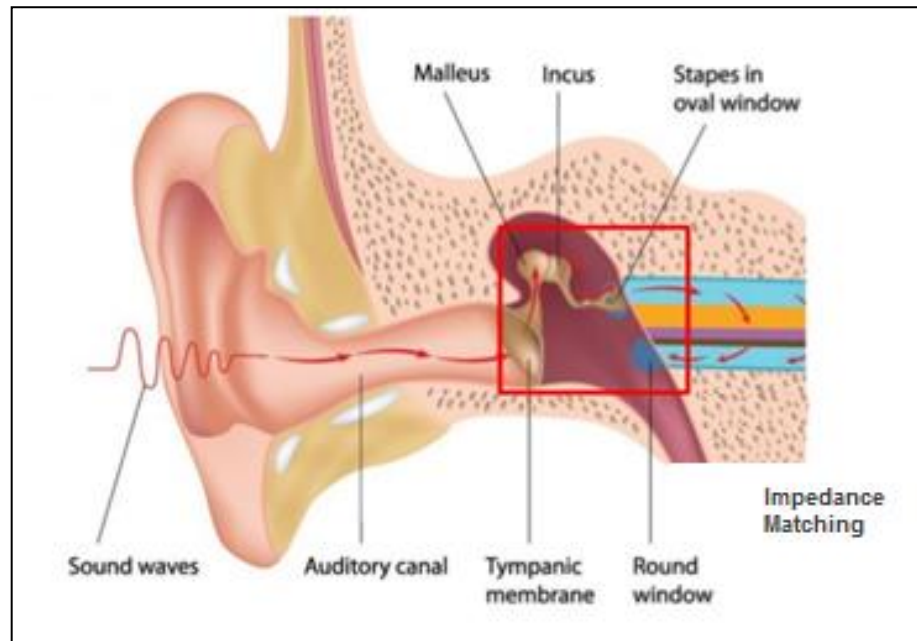


Figure 2.17 Impedance matching layer by the bones in middle ear part of human ear [13].

This impedance matching principle is used in both loudspeakers and musical instruments as well. Most loudspeaker systems include impedance matching mechanisms, especially for low frequency sound waves. The reason is the mismatch of driver impedances to the impedance of free air at low frequencies. Sound from a loudspeaker is relevant to the ratio of the diameter of the speaker to the wavelength of the sound being reproduced. That's why larger speakers can generate lower frequency sound waves at a higher level than smaller speakers.

2.5. Acoustic Meta-materials

Acoustic meta-materials have very unique properties of sound like transmission, absorption and orientation which are not possible with natural materials. These features are provided by their repeating constructions and various configurations

(Figure 2.18). Acoustic meta-materials are consisted of solids and liquids which are embedded in the mediums of solids, liquids and gases.

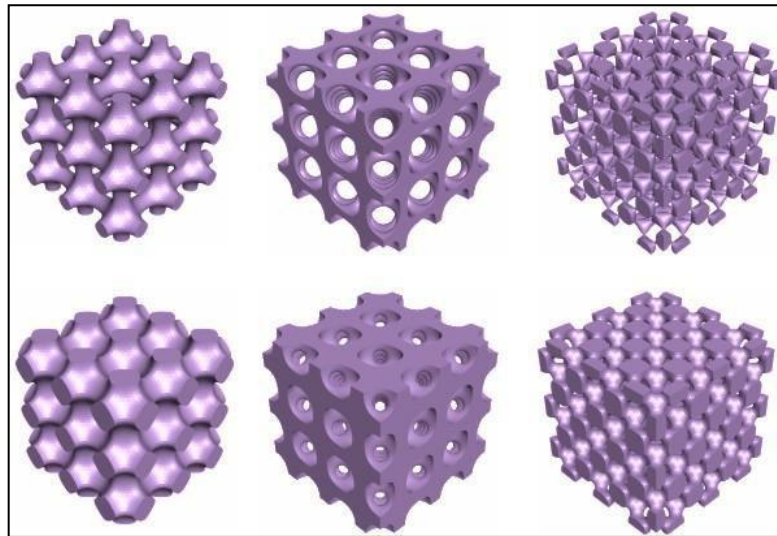


Figure 2.18 Cubical acoustic meta-material samples.

They must at least contain two different materials which will provide periodicity that makes the structure called meta-material. The working mechanism of acoustic meta-materials can be explained by interactions and the scatterings inside the structure as well as the local resonance of each individual (Figure 2.19).

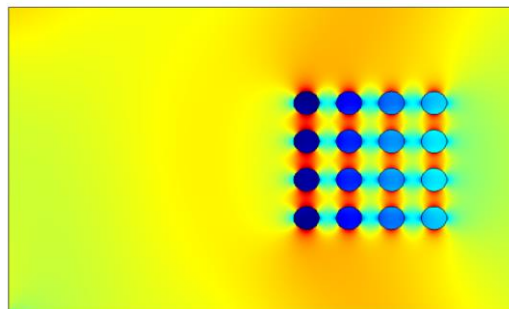


Figure 2.19 Illustration of local resonances and the scatterings seen in the pressure pattern of meta-material structure.

The most significant results of those acoustic interactions between the meta-materials and the incoming sound waves are band gap formations that occur during the propagation of the wave. Band gaps can be basically explained as a property of a meta-material that prevents phonons (A unit of vibration energy that arises from oscillating atoms within a crystal[14].) from being transmitted through the material for a

specific range of frequency. And as expected, these frequency ranges which prevent sound transmission varies according to the physical and geometric properties of the structure. Additionally, even these structures are not very popular in commercial use, they have a wide range of possible applications such as manufacturing sound proof windows [15], providing acoustic cloaking and invisibility [16], [17], designing noise barriers [18] and even building earthquake proof homes [19] in the near future.

2.5.1. History

Acoustic meta-material structures or phononic crystals are first presented in 1990 by Sigalas and Economou who later demonstrated the existence of band gaps in three-dimensional structures [20]. After that, in 1995, Francisco Meseguer and colleagues determined experimentally the aural filtering properties of a perfectly real but fortuitous phononic crystal, a sculpture by Eusebio Sempere standing in a park in Madrid, Spain (Figure 2.20). Sculpture was a two-dimensional periodical square arrangement of steel tubes in air. They showed that attenuation of acoustic waves occurs at certain frequencies [21].

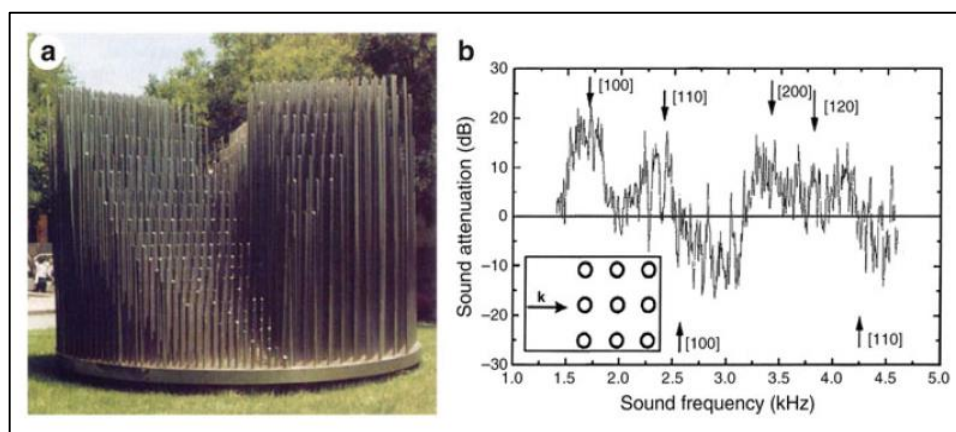


Figure 2.20 (a) Eusebio Sempere's sculpture in Madrid, Spain, (b) Measured sound attenuation as a function of frequency [21].

In 2000, the theory and experimental results of a set of sonic crystals that generate spectral gaps with lattice constants two orders of magnitude smaller than the

relevant sonic wavelength are presented [22]. The reason of the existence of band gaps in these acoustic meta-materials was due to the effect of local resonance in sonic structures. Because the wavelength of sound is very large when compared to the lattice constant of the structure, periodicity is not needed for the gap formation. In this study, a cubic crystal consisting of a heavy solid core material (lead) coated with elastically soft material (silicone elastomer) is used which are embedded in an epoxy matrix (Figure 2.21).

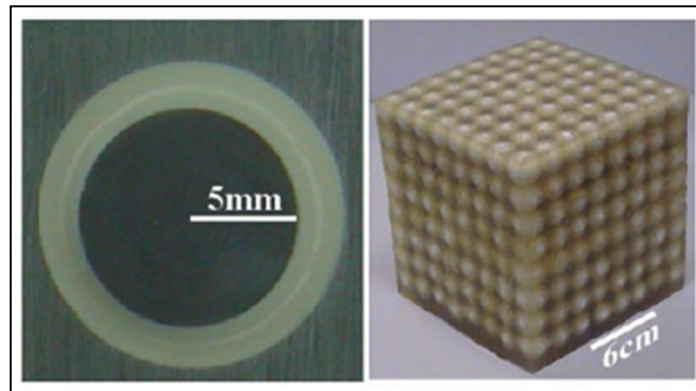


Figure 2.21 Cross section of a coated lead sphere and the illustration of 8x8x8 cubical structure [22].

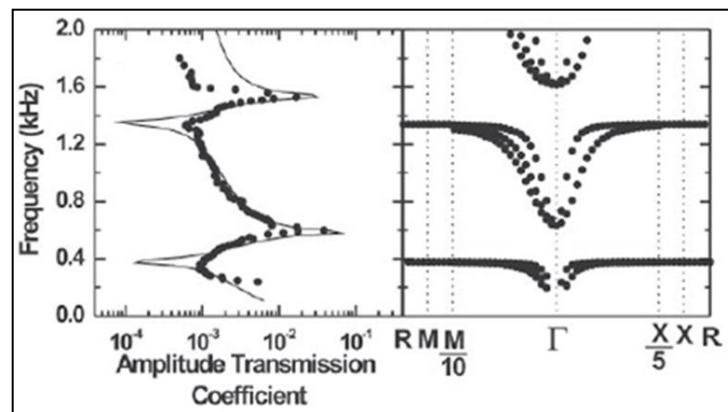


Figure 2.22 Calculated (solid line) and measured (circles) amplitude transmission coefficient along the [100] direction as a function of frequency on the left, and calculated band structure of a simple cubic structure of coated spheres on the right [22].

Small sized (Relative to the wavelength) structures produce very narrow transmission gaps for low frequency sound waves due to the resonances of spherical resonators. The study showed that for specific frequency ranges, sound transmission is permitted through the structure (Figure 2.22).

2.5.2. Geometries

An acoustic meta-material structure may include various types of shapes, arrays and geometric properties. This section includes geometric properties of most common meta-material structure.

2.5.2.1. Individual Elements and Geometries of the Structures

An acoustic meta-material structure consist of individual elements which have various geometric shapes. These geometries contain cylinders [23]–[27], squares [23], eclipses, cubes, spheres [22] and other shapes (Figure 2.23) [28], [29]. Each element correspond to a unit cell that generates the meta-material structure when combined as an array. As for the array formation, common schemes are square, cubical [22], hexagonal [24] and triangular [30].

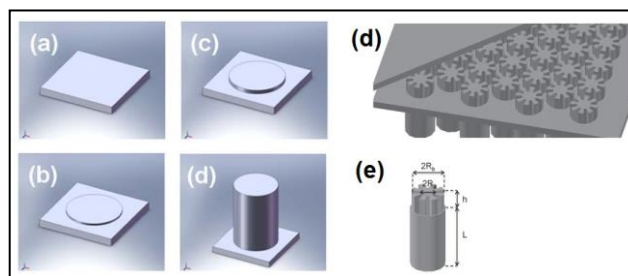


Figure 2.23 Examples for the other shapes of acoustic meta-material elements.

2.5.2.2. Materials

Typically acoustic meta-material structures can be classified as two phase and three phase in terms of materials. Two phase meta-material structures contain two different materials, like steel blocks embedded in epoxy [28] or array of cylindrical holes drilled into the matrix [27]. But most of the time, meta-material structures consist of three different materials (Figure 2.24) which makes them called as three phase [22]–[24], [26], [31], [32].

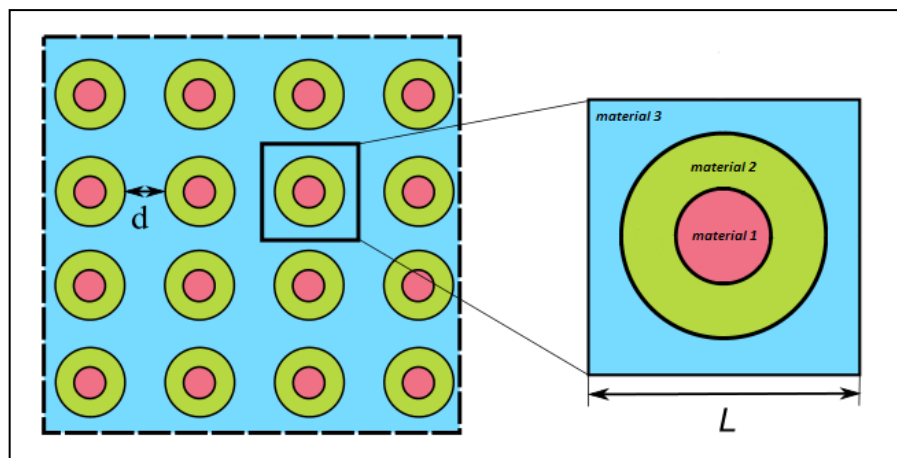


Figure 2.24 Illustration of a three phase meta-material structure.

Individual elements have core materials like steel, tungsten, lead, gold coated with softer materials like silicone rubber, foam and etc. The matrix that holds these elements are generally materials like epoxy, and various kinds of foams. Some noise barriers have no material for the elements to be embedded in, which is an array of individual elements only [33], [34].

2.5.2.3. Applications

Acoustic meta-materials can serve for a wide range of purposes in many different applications. Acoustic cloaking [16], [17], [35]–[38] providing acoustic

invisibility is an extremely important field for radar systems and military technologies (Figure 2.25). Sonic wave guides [39], sound proof windows [15], noise barriers [40], [41], sound absorbers [42], diffusers [43] are other application fields for the industry. All these applications are based on tunable frequency range corresponding to the purpose of the composition.

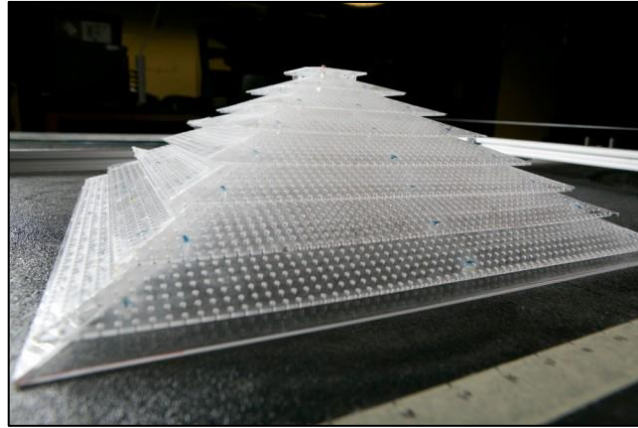


Figure 2.25 World's first 3-D acoustic cloaking device hides objects from sound.

2.5.2.4. Performance

Acoustic meta-material structures have a wide range of geometric, structural and physical properties for fulfilling the required purpose. In general, it can be said that the scale of the structure is inversely proportional to the frequency range desired to have a band gap. It is shown that small sized structures produce very narrow transmission gaps for low frequency sound waves due to the resonances of spherical resonators [22]. In addition to that, coating parameters of the each element which are embedded in the matrix is also effective for adjusting the band gap [24]. In another study it was shown that meta-materials with either periodic or non-periodic arrangements of inclusions have the same dispersion values, which shows that the local resonances of inclusions are influential in this design. Also it is required to provide the enough distance between the inclusions such that they are not too close to avoid coupling effects. It is also possible to increase the number of band gaps by using different sized inclusions. In addition to

those, as it was mentioned before, the coating thickness or the outer radius of the inclusions give chance to make band gap frequencies tunable [23].

2.6. Meta-material Absorbers

Ordinary sound absorbers achieve their sound absorbing properties from the materials they are made of, which are usually soft and porous materials like sponge and mineral wool that have good absorbing properties. Being effective absorbers, these materials absorb sound almost equally from every direction, and the acoustic properties can be called as isotropic. In the applications where the unidirectional sound source's location is important and the source of the noise comes from another direction, these old school sound absorbers cannot distinguish the desirable and undesirable sound. Another negative aspect of traditional sound absorbers is, they are opaque and cannot be used when transparency is needed and in addition to those, being limited to physical properties of those natural materials, which make the sound absorbers unable. However, in the last few years, new types of materials are developed which are called as acoustic meta-materials, they have unique tunable sound propagation and absorption properties. Variation of absorption properties of an example structure according to the directions are illustrated in Figure 2.26. It shows that absorber is able to behave in different ways against the sound waves incoming from diverse directions.

Another study focuses on sound absorption under-water in which the absorption is in very narrow frequency range around the resonance frequency. To improve that, usage of several acoustic meta-material layers each has different resonant frequencies is presented. In the experiment, main material was a type of styrene butadiene rubber, and the soft coating which is made of two-component, room temperature vulcanizing silicone rubbers (RTV-2). Experimental and numerical results show that the broadband sound absorber with two layers produces a better performance than one type of local resonance scattering structures [42].

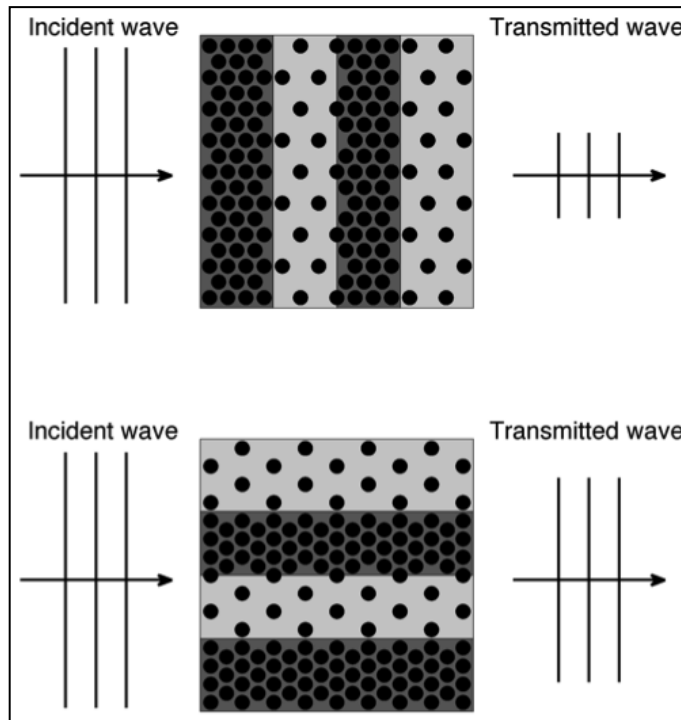


Figure 2.26 Different sound absorption properties in different directions [44].

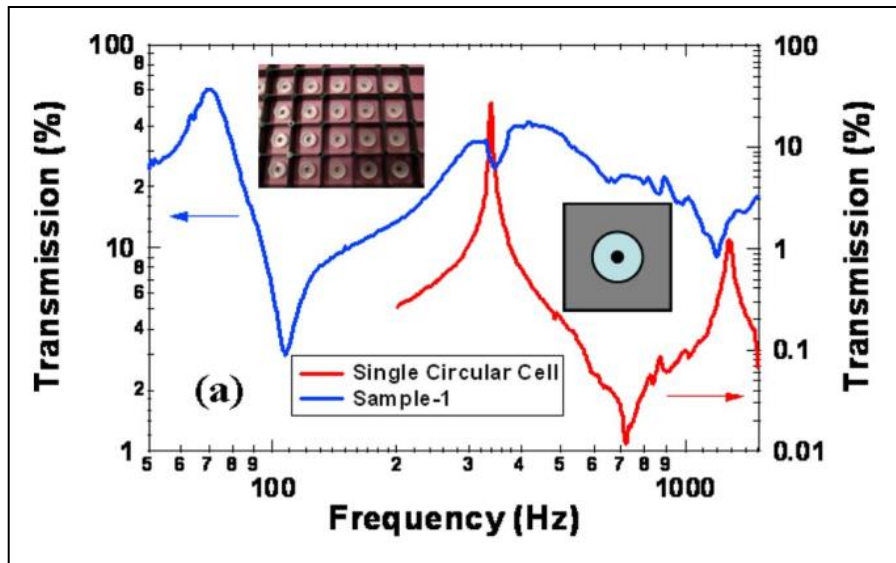


Figure 2.27 Transmission spectrum of a single circular cell (red curve) with an attached mass of 0.11 g, and Sample-1 (blue curve) with an attached mass of 0.71 g. The left hand inset shows the front view of a planar array of square unit cells. The right hand inset shows the front view of a single circular cell [48].

Control of low frequency noise is a problem as discussed previously, due to its high penetrating power. Brick or concrete walls usually provide noise attenuation at frequencies above 500 Hz which can be classified as mid to high frequency ranges. But

around 100 Hz their effectiveness is very low [18], [45]–[47]. Another study is based on a membrane-type acoustic meta-material consists of a thin membrane fixed by a rigid plastic grid, with a small mass add on at the center of each grid (Figure 2.27).

Sample-1 has an attached mass of 0.71 grams. Sample-2 and Sample-3 are similar to Sample-1, but the attached mass is different, which is 0.21 grams. The STL curve of the two samples, measured alone, are shown in Figure 2.27 as the red and the green curves. The blue curve denoted as Sample-(2+3) in Figure 2.28, is the STL spectrum sample formed by stacking Sample-2 and Sample-3 together. Four single-layer panels with proper stop bands were selected to generate a broadband attenuation shield. The first one contains a single weight and the second one contains four weights per four-in-one cell. The third one contains two 0.52 g weights. The fourth and the last one contains a single weight of 0.52 g. The total thickness is 60 mm and the total weight is 15 kg/m². The purple curve in Figure 33 shows the measured STL for the multi-layer panel [48]. The results showed that a broadband sound shield, comprising simple stacking of membrane-type meta-materials are operative for wider frequency ranges.

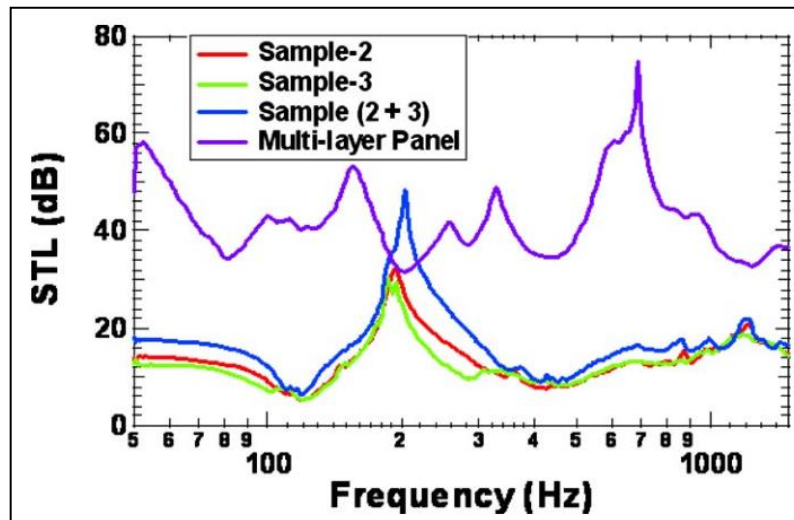


Figure 2.28 The STL spectra of two nominally identical single-layer samples (red and green curves), together with the STL spectrum measured from the stacking of the two samples (blue curve). The purple curve is the STL spectrum of a broadband shield consisting of four single-layer panels [48].

CHAPTER 3

FINITE ELEMENT MODELING

In the simplest form, mathematical solution methods can be classified into analytical and numerical methods. In numerical methods, finite element method is frequently used in acoustics. In this study both finite element and analytical methods which are explained in detail are used for analyzing the sound absorption characteristics of the sound absorbing structures. Impedance transfer methods are employed in both for modeling the system based on defining the acoustic impedance values of absorber layers and the surfaces.

3.1. Acoustic Impedance

Basically Acoustic impedance and the specific acoustic impedance can be explained both as the measures of the reaction that a system gives to the acoustic flow. Specific acoustic impedance is simply the acoustic impedance of the surface, which is also known as surface acoustic impedance. The SI unit of acoustic impedance is the Pascal second per cubic meter ($\text{Pa}\cdot\text{s}/\text{m}^3$) or the Rayl per square meter (Rayl/m^2), while that of specific acoustic impedance is the pascal second per meter ($\text{Pa}\cdot\text{s}/\text{m}$) or the rayl. In general form, both acoustic impedance and specific acoustic impedance can be written as a complex value – Z :

$$Z = X + jM \quad (3.1)$$

where X is the acoustic resistance and M is the acoustic reactance. Resistance can be explained as the loss, due to various mechanisms, mostly by thermal dissipation, and reactance is the ability of medium or layer to store energy of the incoming sound wave. The absolute value of the characteristic specific acoustic impedance of a layer can also be expressed as – Z_i :

$$Z_i = \rho C \quad (3.2)$$

Where ρ as the density (kg/m^3) and C as the sound velocity (m/sec) in the corresponding layer.

3.2. Empirical Model for Porous Absorber

Empirical model for porous absorption is based on Delany and Bazley model and the corresponding coefficients to define the characteristic impedance of any porous layer [49]. The equation of the characteristic impedance of the porous layer— Z_i , and the complex specific propagation constant— Γ_i , are shown below respectively:

$$Z_i = Z_0(1 + c_1X^{c_2} - jc_3X^{c_4}) \quad (3.3)$$

$$\Gamma_i = \frac{w}{c_0}(c_5X^{c_6} + j(1 + c_7X^{c_8})) \quad (3.4)$$

The term X is an empirical parameter without any physical meaning, which can be defined:

$$X = \rho_0 f / \sigma \quad (3.5)$$

where ρ_0 is the density of air, f is the frequency and σ is the airflow resistivity of the layer. To obtain the surface impedance of the corresponding layer — Z_s , the equation below should be used, where l is the thickness of the absorbent material.

$$Z_s = Z_0 \coth(\Gamma_i l) \quad (3.6)$$

To attain the absorption coefficient, complex reflection factor(dimensionless) must be known, and it can be expressed as:

$$R = Z_s - Z_0 / Z_s + Z_0 \quad (3.7)$$

Then the absorption coefficients can be obtained as:

$$\alpha = 1 - |R|^2 \quad (3.8)$$

3.3. Standing Wave Ratio(SWR) Method

Standing wave ratio method is based on ratio of pressure maximum (anti-node) to pressure minimum (node) as shown below (Figure 3.1).

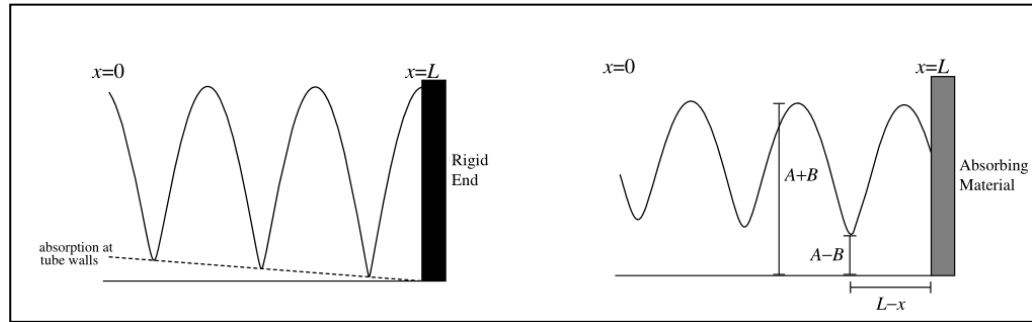


Figure 3.1 Illustration of minimum and maximum pressure values.

The amplitude at a pressure anti-node (maximum pressure) is $(A+B)$, and the amplitude at a pressure node (minimum pressure) is $(A-B)$. It is not possible to measure A or B directly but it is possible to obtain $(A + B)$ and $(A - B)$ using the standing wave tube or finite element simulation. The ratio of pressure maximum to pressure minimum as the standing wave ratio is defined as below:

$$SWR = A + B/A - B \quad (3.9)$$

The sound absorption coefficient depending on the SWR is expressed as:

$$\alpha = 1 - [(SWR - 1)^2/(SWR + 1)^2] \quad (3.10)$$

The SWR method is based on obtaining the maximum and minimum pressure values for each frequency which is studied. However this method does not work well if the tube length you are modeling is not long enough, especially for lower frequencies. Since it is known that a low frequency means a longer wave length, if the measure of the tube which is used is not fulfilling at least the longest wave length that the sound wave is propagating corresponding to the lowest frequency included in the model, it won't be assured that you will have the maximum or minimum pressure values will be

included in the pressure profile you have taken from your solved model. Choosing the right length for the pressure profile is shown below (Figure 3.2).

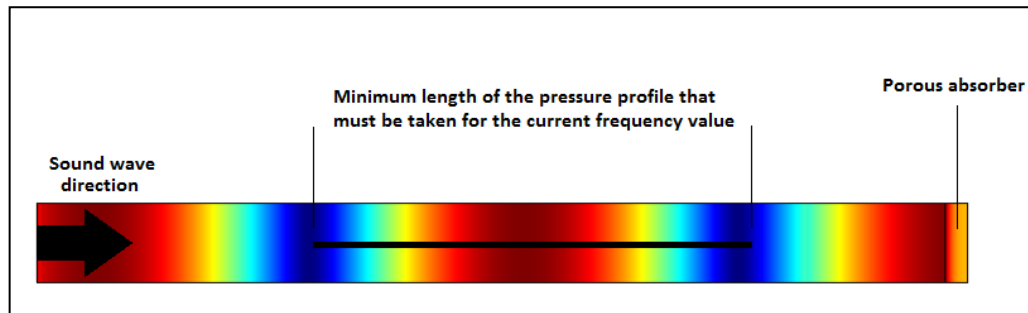


Figure 3.2 Example of the minimum length of the pressure profile that must be taken to obtain SWR

3.4. Transfer Matrix Method

Transfer matrix method, is commonly used in acoustic problems for obtaining absorption characteristics of multi layer acoustic absorbers. In this study, transfer matrix method is used to evaluate impedance and absorption characteristics of the corresponding sound absorber. Transfer matrix defines surface impedances of the layers by using characteristic impedance Z_l of the layer and propagation constant γ .

General solution of a plane wave traveling in air is simply given as;

$$p = A \exp\left\{j\omega\left(t - \frac{x}{c_0}\right) - \kappa x\right\} \quad (3.11)$$

where A is a complex constant, ω is the angular frequency c_0 is the speed of sound in air and κ is the attenuation constant.

Acoustic pressure of $p(0)$ at $x = 0$ can be written as:

$$p(0) = A \exp \{j\omega t\} \quad (3.12)$$

At $x = 0$, pressure of the plane wave as a function of x can be found using Equations 3.11 and 3.12 as:

$$p = p(0) \exp\{\gamma x\} \quad (3.13)$$

An expression for flow velocity can be written like pressure expression:

$$v = v(0) \exp\{\gamma x\} \quad (3.14)$$

where propagation constant γ is defined as complex sum of attenuation constant and phase constant β : $\gamma = \kappa + j\beta$ and $\beta = \frac{\omega}{c_0}$

For the derivation of the transfer matrix formulation, assumption of a layer l with characteristic impedance Z_l is made. The surface acoustic impedance at the bottom of the layer is given by Z_1 at $x=0$ as a result of previous layer, surface impedance Z_2 at $x=l$ resulting from Z_1 and Z_l , incident plane wave P_i and plane wave reflected from the boundary at $x=0$ P_r .

Impedance (specific acoustic impedance) as a function of x is expressed as:

$$Z(x) = \frac{p(x)}{v(x)} \quad (3.15)$$

In the layer 1, pressure at any point x can be obtained by superposition of the pressures resulting from the incident and the reflected waves as:

$$p(x) = P_i \exp(\gamma(l-x)) + P_r \exp(-\gamma(l-x)) \quad (3.16)$$

Similarly particle velocity at any point x by vectoral sum of particle velocities of incident and reflected waves can be obtained as;

$$v(x) = \frac{P_i}{Z_l} \exp(\gamma(l-x)) - \frac{P_r}{Z_l} \exp(-\gamma(l-x)) \quad (3.17)$$

At the boundary interface $x = l$, inside the layer l , surface impedance Z_2 can be found as;

$$\frac{p(l)}{Z(l)} = Z_2 \quad (3.18)$$

Also, total pressure and particle velocity of incident and reflected wave at $x = l$ is;

$$p(l) = P_i + P_r \quad (3.19)$$

$$v(l) = \frac{P_i}{Z_l} - \frac{P_r}{Z_l} \quad (3.20)$$

Using Equations 27, 28 and 29, magnitude of the reflected wave can be found as:

$$P_r = P_i \frac{Z_2 - Z_l}{Z_2 + Z_l} \quad (3.21)$$

Putting Equations 3.21 into Equations 3.16 and 3.17; expressions for pressure and velocity at $x = 0$ can be obtained as follows:

$$p(0) = P_i \exp(\gamma l) + P_i \frac{Z_2 - Z_l}{Z_2 + Z_l} \exp(-\gamma l) \quad (3.22)$$

$$v(0) = \frac{P_i}{Z_l} \exp(\gamma l) + \frac{P_i}{Z_l} \frac{Z_2 - Z_l}{Z_2 + Z_l} \exp(-\gamma l) \quad (3.23)$$

At the boundary interface $x=0$, inside the layer l , surface impedance Z_1 can also be defined as:

$$\frac{p(0)}{v(0)} = Z_1 \quad (3.24)$$

Inserting Equations 3.22 and 3.23 into Equation 3.24 and rearranging terms, the expression for resulting surface impedance Z_1 at $x=l$ can be obtained as a function of surface impedance Z_2 at $x=0$, impedance of layer Z_l and propagation constant γ as:

$$Z_1 = Z_l \frac{Z_2 \cosh(\gamma l) + Z_l \sinh(\gamma l)}{Z_2 \sinh(\gamma l) + Z_l \cosh(\gamma l)} \quad (3.25)$$

As a specific case, when any layer is backed by a rigid wall, the impedance Z_2 is thought to be infinite.

When $Z_2 \rightarrow \infty$, impedance at the top of the layer can be evaluated as:

$$Z_1 = Z_l \coth(\gamma l) \quad (3.26)$$

In this study, transfer function is defined as H_{12} , ratio of complex pressure values obtained from microphone position 1 to position 2, which can be written as p_2/p_1 . H_{12} is a complex number as it is understood from the definition. This ratio can be obtained by measuring the sound pressure values for the required frequencies by any experimental setup (Figure 3.3) that contains impedance tube and a material sample or a finite element model.

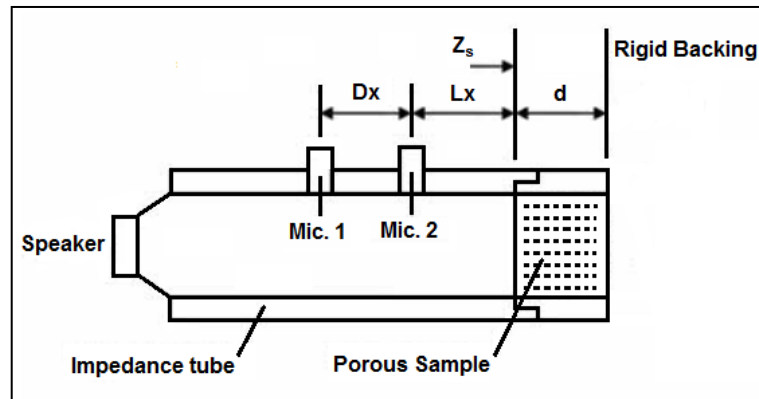


Figure 3.3 Schematic diagram of an experimental impedance tube setup.

The surface acoustic impedance of the layer is then obtained by equation below:

$$Z_s = \frac{\{H_{12} \sin[k(Lx+Dx)] - \sin(kLx)\}}{\{\cos(kLx) - H_{12} \cos[k(Lx+Dx)]\}} \quad (3.27)$$

After obtaining the surface acoustic impedance, the same steps are applied as in the theory, complex reflection factor – R is being calculated and then the sound absorption coefficients – α of the absorber are defined by using equation 17.

3.5. Finite Element Model

3.5.1. Comsol Multiphysics 5.0

Comsol Multiphysics is a finite element package which is commonly used in many fields of engineering. Wide application area of the software allow users to analyze various kinds of engineering problems including pressure acoustics, heat transfer, structural mechanics, heat flow, optics and more.

3.5.1.1. Acoustics module

The Acoustics Module of the software provides users an opportunity to solve many different kinds of acoustic problems in the manner of finite elements. In the Acoustics Module, Comsol presents four different model types including pressure acoustics, acoustic-structure interaction, aero-acoustics and thermo-acoustics. In this study, pressure acoustics option is used for obtaining the absorption characteristics of the corresponding structure.

3.5.1.2. Generating the model

Before generating the unique finite element model with the locally resonant inclusions, only an absorber containing structure is modeled and solved to see and determine if the methods are working fine. Verification model (Figure 3.4) was a porous absorber with a wool material which has a thickness of 18 mm with a rigid backing [49]. By using the transfer function method, complex pressure values are obtained in finite element model generated in Comsol, and then those pressure values are used to run the prepared Matlab codes to obtain the absorption coefficients of the absorber (Figure 3.5).

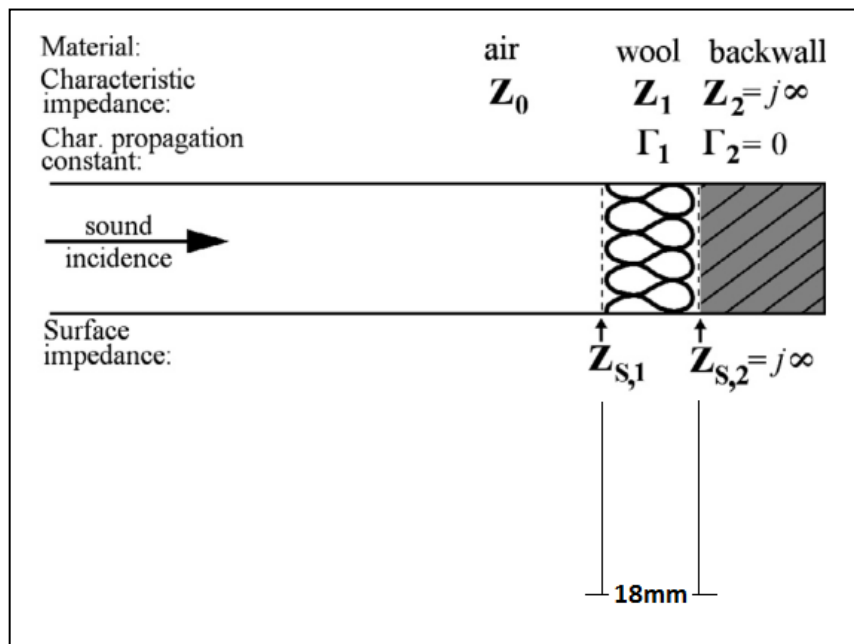


Figure 3.4 Schematic illustration of the setup[49].

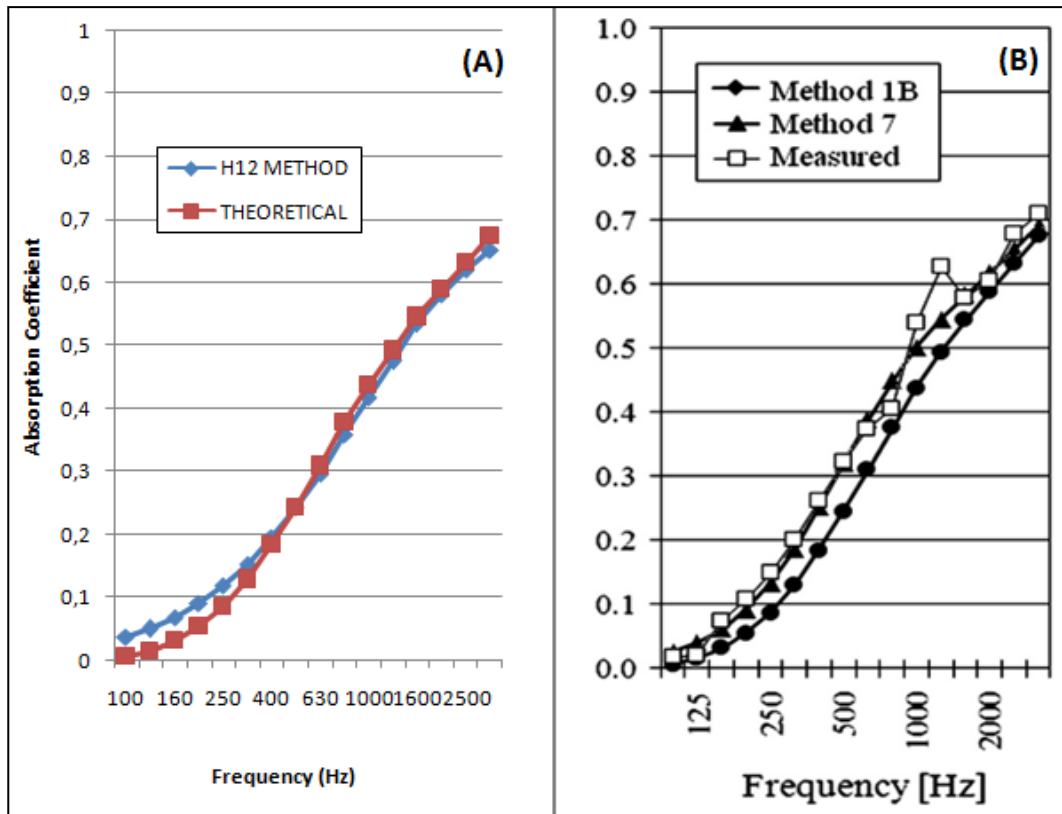


Figure 3.5 (A) Absorption coefficients obtained by finite element method and theory, (B) Absorption coefficients obtained by Oliva D. and Hongisto V., 2013 [49].

3.5.1.3. Geometry

The geometry of the considering structure in this study consists of a tube which has a length of 20cm and an absorber at the end with the thickness of 50mm with rigid backing. After the generation of the basic geometric entities, cylindrical blocks with various properties are embedded in the porous absorber. Since it is known that 3D modeling requires longer computation process when compared to 2D modeling, it is decided to generate the same model both 2D and 3D to see if it is possible to use 2D models to save time and make more parametric variations and trials. After the agreement of the results shown below, models are generated in 2D (Figure 3.6).

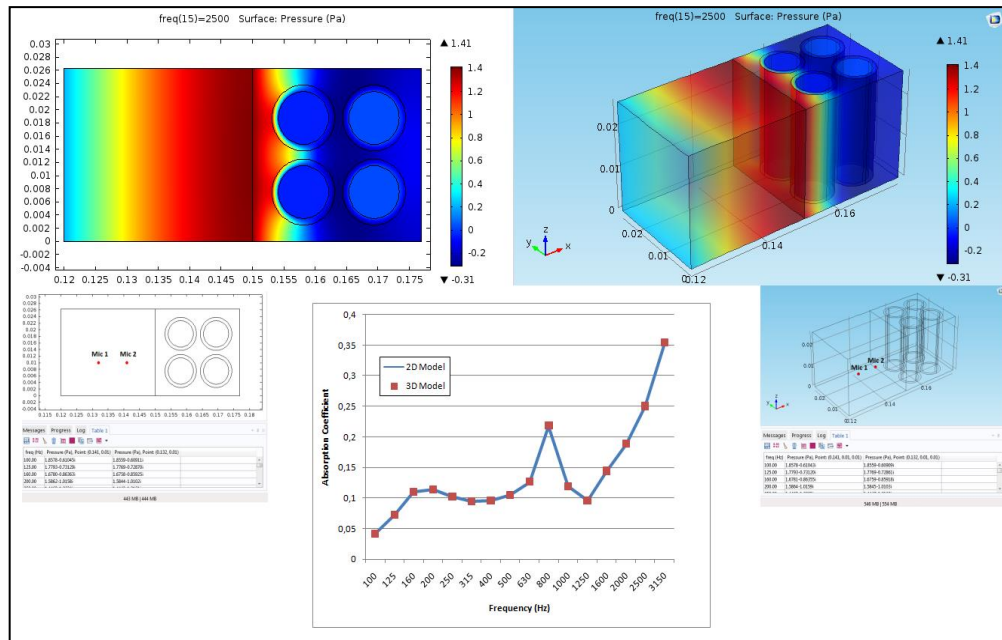


Figure 3.6 Comparison of the absorption coefficients obtained by 2D and 3D models.

3.5.1.4. Material properties

In the model background domain is defined as air with the density of 1.204 g/cm^3 and the sound velocity of 344 m/sec . Porous absorber is defined by Delany and Bazley coefficients (Table 3.1) and with the air flow resistivity of 215000 Pa.s/m^2 . Additional cylindrical blocks are modeled as various material types, some of them are already found in the Comsol material library. These coefficients correspond to the ones used in equation 12 and 13.

Table 3.1 Delany and Bazley Coefficients[49].

C_1	C_2	C_3	C_4	C_5	C_6	C_7	C_8
0.05710	-0.75400	0.08700	-0.73200	0.18900	-0.59500	0.09780	-0.70000

3.5.1.5. Initial conditions

The default temperature of 293.15 K is applied and incident plane waves are perpendicularly (+x direction) sent to the absorber with the pressure amplitude of 1 Pascal, 1/3 Octave band frequencies are chosen to study, and 100 Hz – 3150 Hz frequency range is considered.

3.5.1.6. Boundary Conditions

When generating the model, except the boundary condition of the source, all the other outer boundaries are defined as sound hard boundary wall, which does not allow any sound waves to pass through to simulate both the impedance tube and the rigid backing (Figure 3.7).

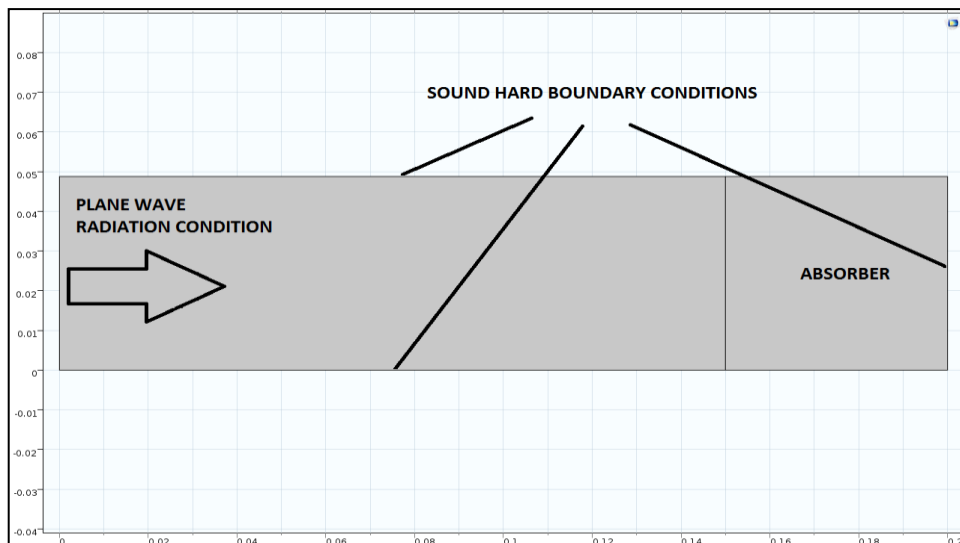


Figure 3.7 Default boundary conditions of the models

3.5.1.7. Meshing

In the meshing process Comsol allows you to choose between various types of mesh elements. In this study both mapped and triangular mesh elements are used (Figure 3.8).

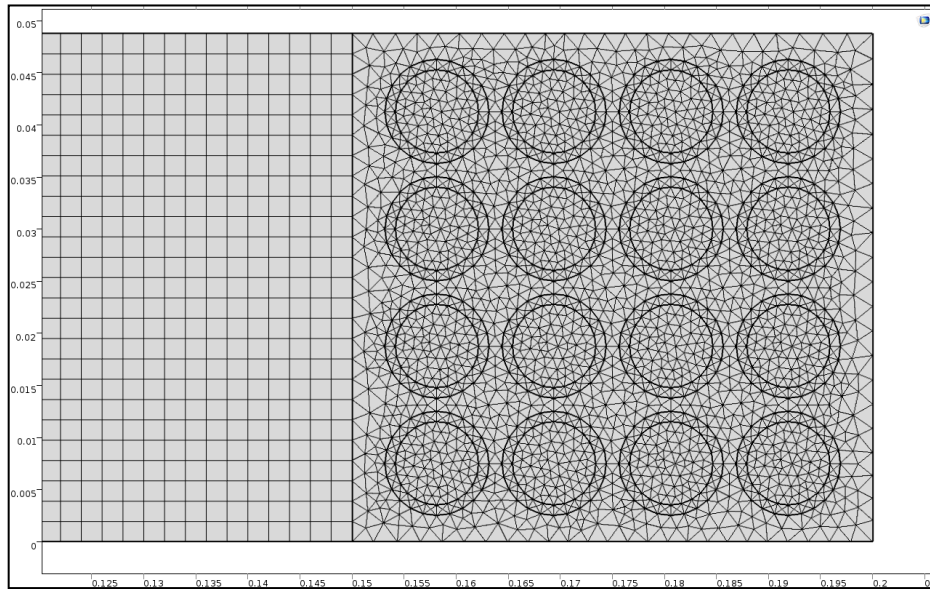


Figure 3.8 Mesh types used in the models.

There are basically two important criteria while meshing the geometry. First one is, meshing the material transition regions as small as possible to have more data points instead of letting the finite element software to interpolate the values in between two nodes. Applying this will result with achieving more realistic data. The second important thing about meshing is choosing the right mesh size. That doesn't mean choosing the smallest mesh size possible since it will result with pretty long computation time but it means choosing the suitable size according to the highest frequency available in the solution. Highest frequency means the smallest wave length the simulation includes. According to the study which is done before, best way is using at least 6 mesh elements per smallest wave length available [50]. In our case the highest frequency value is 3150 Hz, which means the smallest wave length is approximately 109.2 mm. According to the limiting case largest mesh size must be 18.2 mm. In this

study, according to the Comsol interface, normal mesh size is used, which is corresponding to 13.4 mm per the maximum mesh size included in the model.

3.5.1.8. Study

Each model is solved in frequency domain, and in 1/3 Octave band frequencies (Table 3.2) which means there are 16 different frequency values for each model solved for obtaining the absorption characteristics.

3.5.1.9. Obtaining the absorption coefficients

After the model is solved, the next thing to do is reading the pressure values of each microphone placed in the tube. In our case microphone 1 is placed 18mm away from the absorber, and the microphone 2 is placed 18mm away from the first microphone, which means $Dx = Lx = 18$ mm (Figure 3.4). And then absorption coefficients are obtained by using the Matlab codes.

Table 3.2 1/3 Octave Band Frequencies.

<i>Frequency</i>
100 Hz
125 Hz
160 Hz
200 Hz
250 Hz
315 Hz
400 Hz
500 Hz
630 Hz
800 Hz
1000 Hz
1250 Hz
1600 Hz
2000 Hz
2500 Hz
3150 Hz

CHAPTER 4

RESULTS AND DISCUSSION

This chapter contains the models generated in Comsol through a parametric study and the resulting absorption properties. The results and the effects of the parametric and geometric variation are presented and discussed in detail.

4.1. Absorber without the Addition of Cylindrical Elements

Before adding the cylindrical blocks and seeing the effect to the absorption characteristics, the porous absorber without any inclusion is presented. Plane wave radiation condition is applied to simulate an impedance tube to the porous absorber having a thickness of 50mm. Pressure diagram of the model is shown below (Figure 4.1).

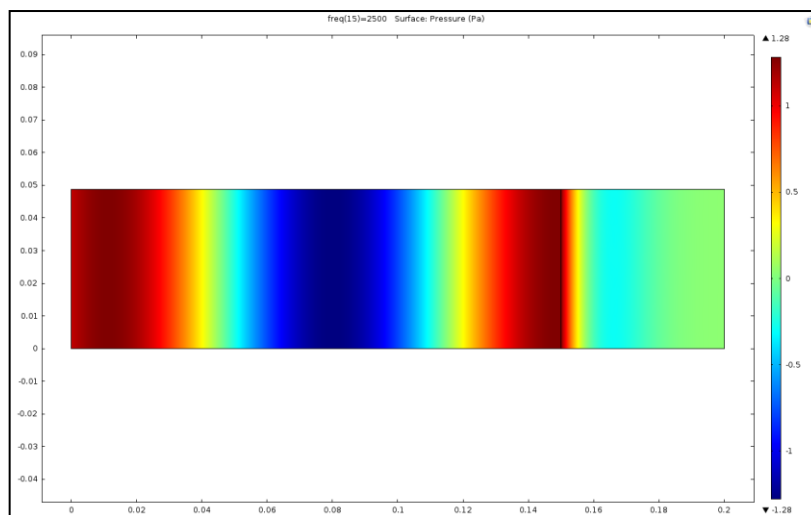


Figure 4.1 Pressure diagram of the model at 2500 Hz without any inclusions.

From the pressure map shown above, absorption coefficients of the porous material are obtained (Figure 4.2).

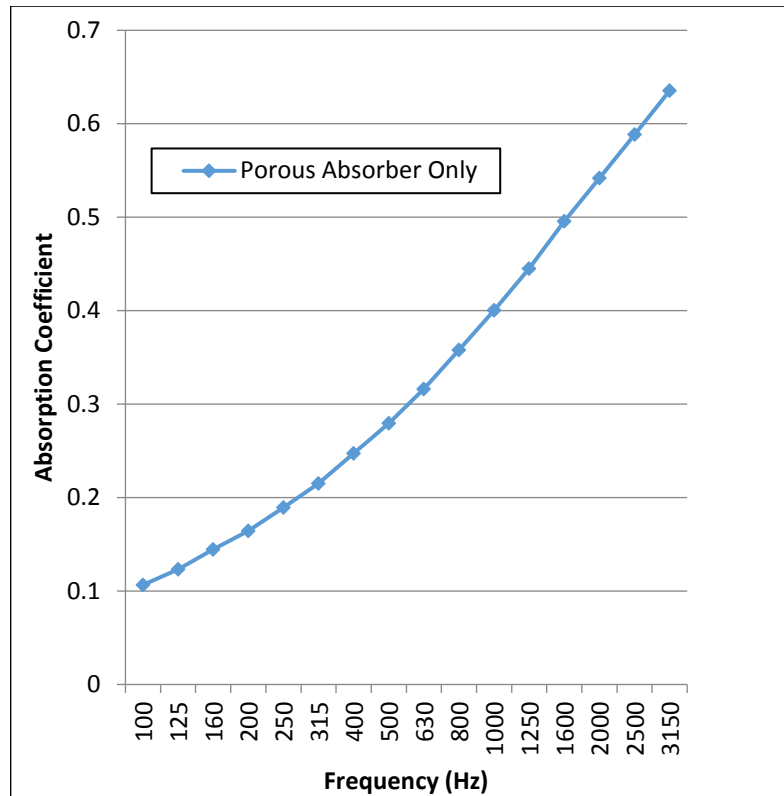


Figure 4.2 Absorption coefficients of the porous media.

The results are quite close to the porous absorber which was modeled to verify the results in the previous sections (Figure 3.5). As it is seen from the curve, absorption coefficients tend to increase, the more you increase the frequency values of the sound.

4.2. Absorber with Cylindrical Holes

Before adding the inclusions, to see the effect of the perforation to the absorption properties, different sized holes are added to the absorber, with the array of 4x4 and defined as air (Figure 4.3). Four different sizes of hole arrays are applied (Table 4.1). Acoustic pressure diagram is shown in Figure 4.4.



Figure 4.3 Schematic representation of the holes.

Table 4.1 Hole diameter variations

<i>Case Number</i>	<i>Hole Diameter</i>
1	1 cm
2	8 mm
3	6 mm
4	4 mm

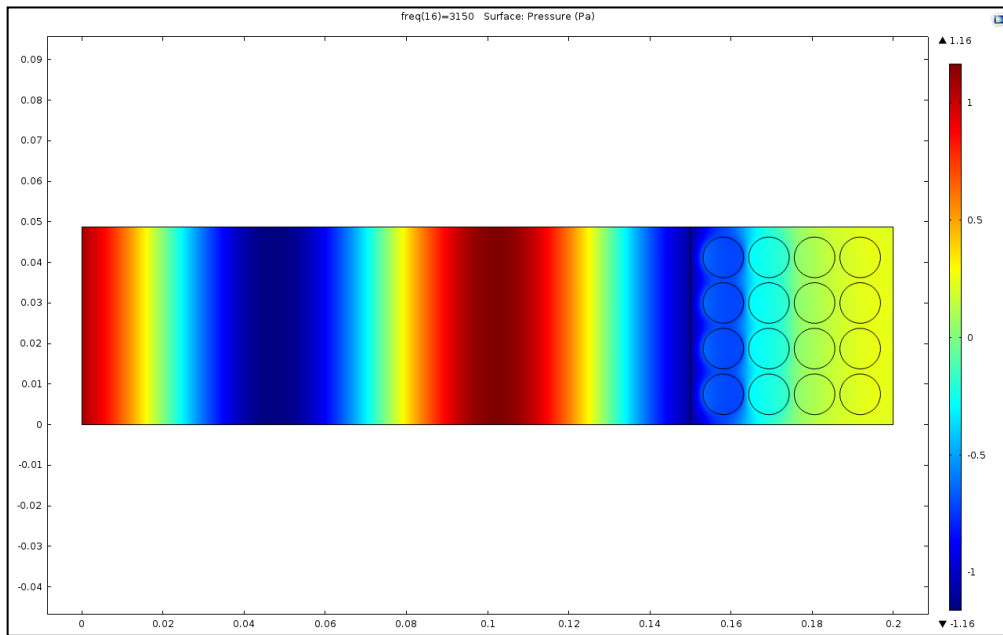


Figure 4.4 Acoustic pressure map of the structure for the frequency value of 3150 Hz.

The results showed that even without adding any materials, drilling some holes to the porous material as an array is resulting with better absorbing properties when compared to an absorber without any holes (Figure 4.5).

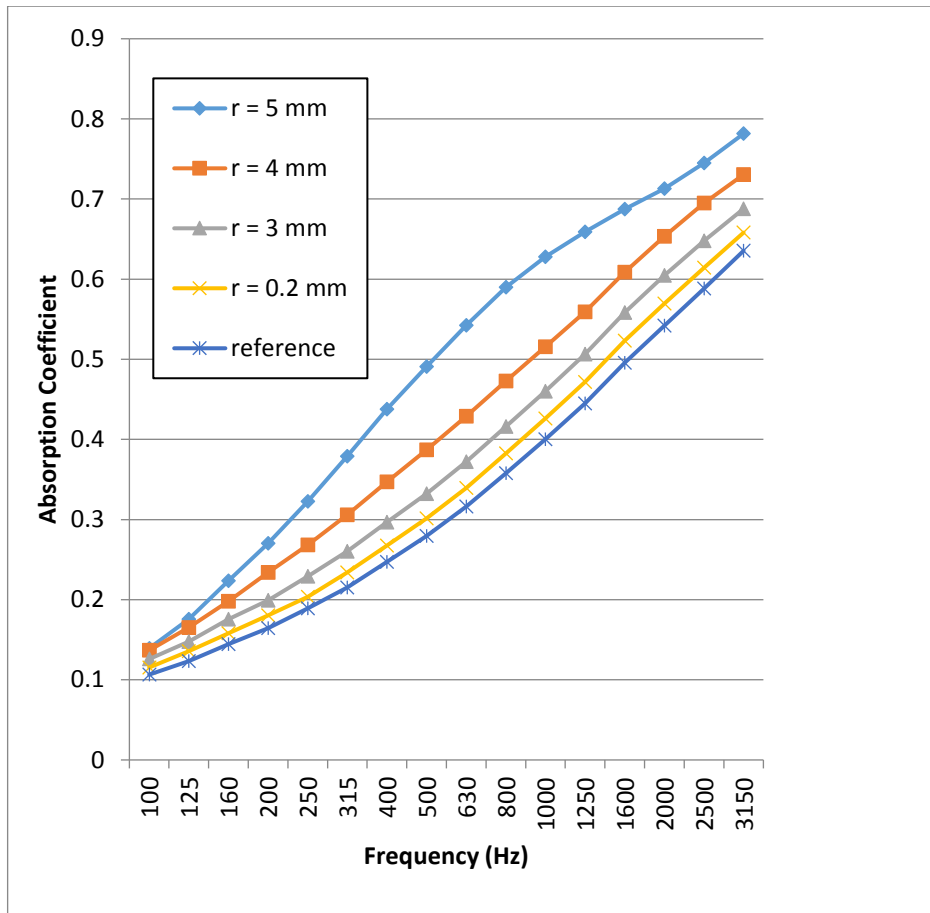


Figure 4.5 Effect of holes to the absorption properties (r is the hole radius).

It is clearly seen that larger hole diameter provide better absorption properties especially in higher frequencies and the best results are taken from the absorber with the hole diameter 1cm.

4.3. Absorber with Different Hole Sizes

In this section, the diameters of the holes are both increased and decreased in the direction of sound propagation to see the effect to the absorption properties. Absorption coefficients are shown in Figure 4.6.

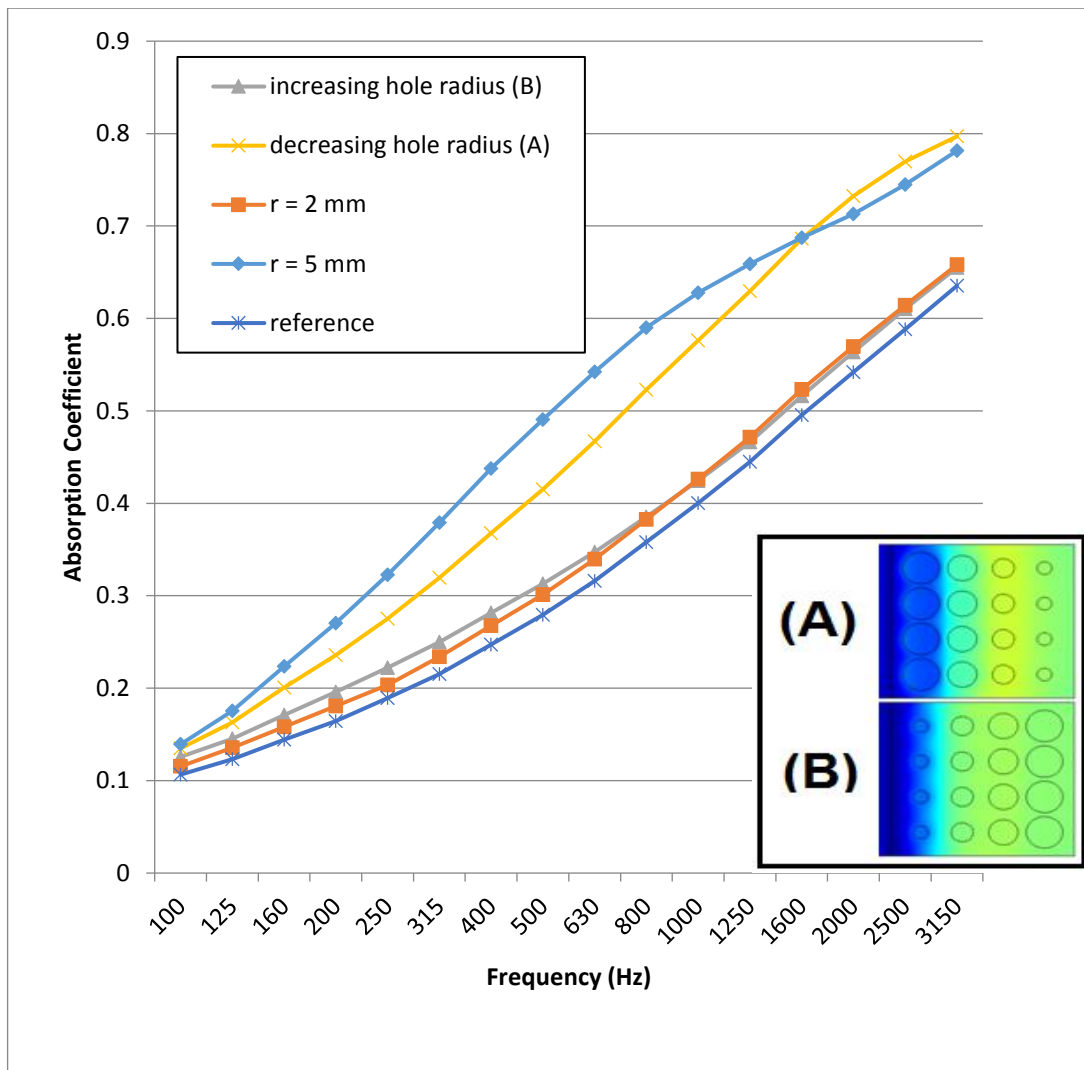


Figure 4.6 Absorption coefficients of two different setups

It is clearly seen that decreasing the hole size in the direction of propagation give better results when compared to the vice-versa. The reason is the gentle increment in the material amount in the direction of sound propagation.

4.4. Absorber with Cylindrical Elements Filled with Foam

Adding inclusions to the porous absorber are divided into two parts. In both parts, different thickness values are applied to see the effect to the absorbing characteristics of the structure and the outer diameter of the cylinders are kept constant,

1cm. At first, inner part of the cylindrical pipes are filled with foam. And next, those pipes will not be filled with any foam material but with air inside which will be presented in the following section. Schematic illustrations of both models are shown above (Figure 4.7).

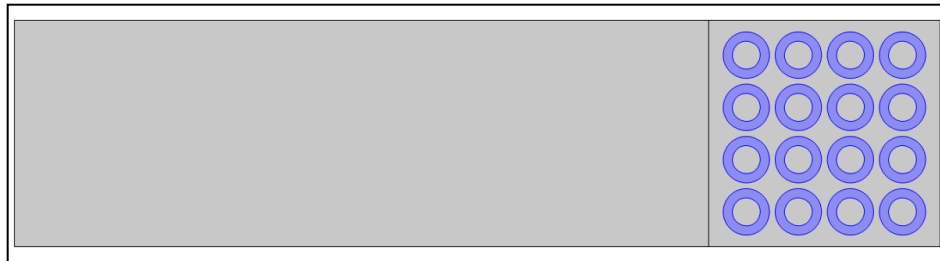


Figure 4.7 Schematic illustration of the model with the pipe thickness of 2mm.

Pressure diagram of the foam filled pipe containing structure is shown below (Figure 4.8). By using the pressure diagram, pressure values for each 1/3 Octave band frequencies are taken to generate the transfer function – H_{12} to obtain the absorption coefficients (Figure 4.9).

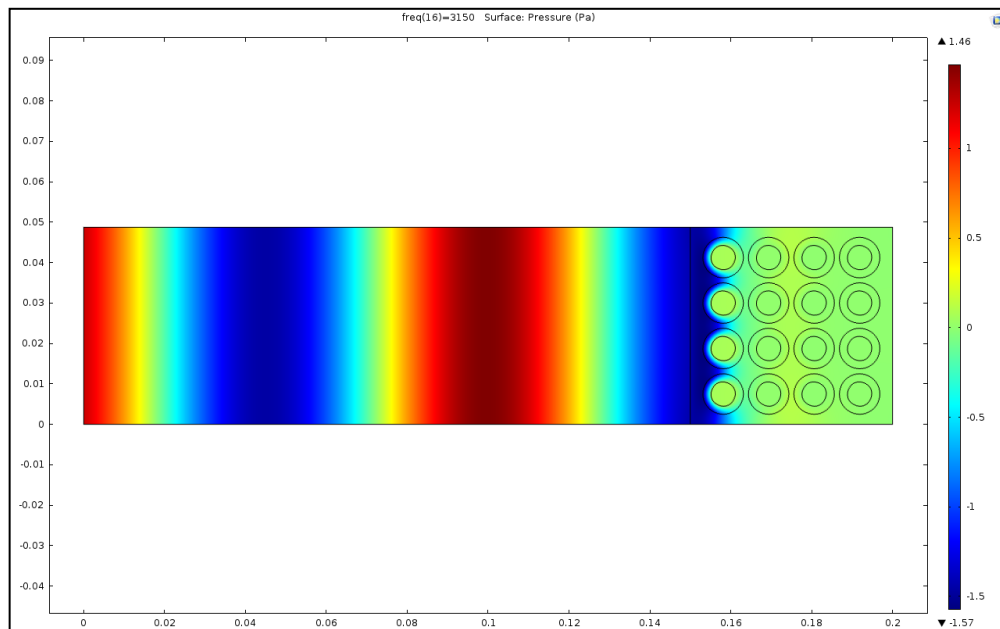


Figure 4.8 Pressure diagram of the foam filled cylinder added model for the frequency of 3150 Hz.

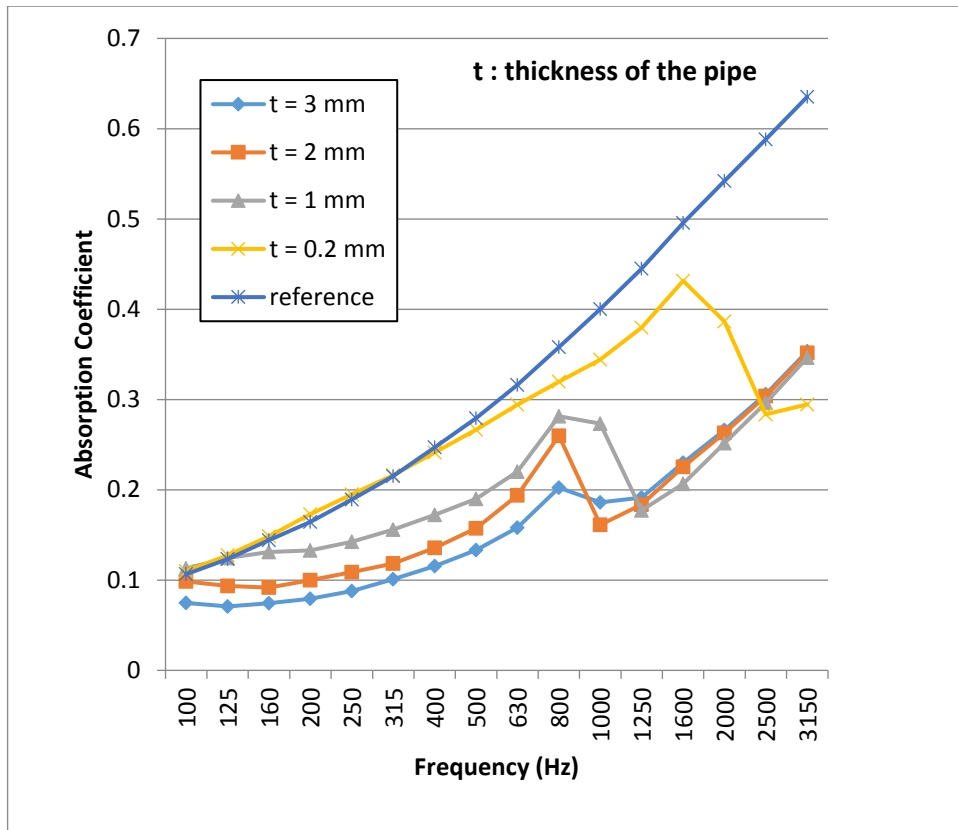


Figure 4.9 Absorption coefficients for the foam filled inclusions with different thickness values.

It can be said that thinner the pipe is, the better absorption properties it will provide. However, these inclusions are not making the absorber more efficient when compared to the no cylindrical blocks added version.

4.4.1. Applying different materials

After seeing that foam filled inclusions are not making a porous absorber more efficient with the aluminum pipe additions, other materials (Table 4.2) are defined in the model instead of aluminum to understand if choosing the right pipe material is an important fact or not.

Table 4.2 Sound velocity and density values of the used materials.

Material	Sound Velocity (m/s)	Density (kg/m³)
Aluminum	5000	2700
Steel	6100	7850
Lead	2160	11340
Glass	3962	2500
Spruce	5278	450

The absorption coefficients obtained from different material types are shown below (Figure 4.10).

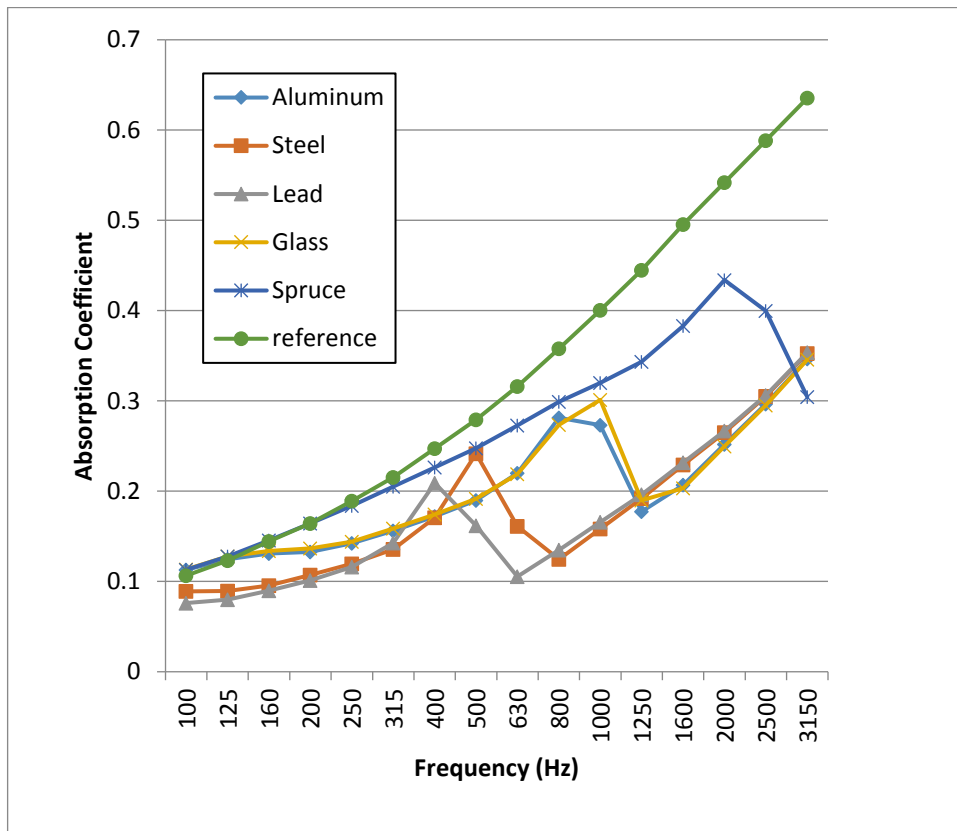


Figure 4.10 Absorption coefficients obtained from different inclusion material types for absorber with the pipe thickness of 1mm and outer hole diameter of 1 cm.

The results showed that changing the foam filled pipe material does not make the absorber more efficient, sometimes makes it even worse. But still we can say that, if the pipe materials you use have closer impedance values, you are going to obtain closer absorption coefficients for these absorbers.

4.5. Absorber with Hollow Cylindrical Elements

In this model, pipes are filled with air and embedded in the porous absorber. Same array and the same thickness values with the section 4.4 are applied. Pressure diagram is obtained (Figure 4.11).

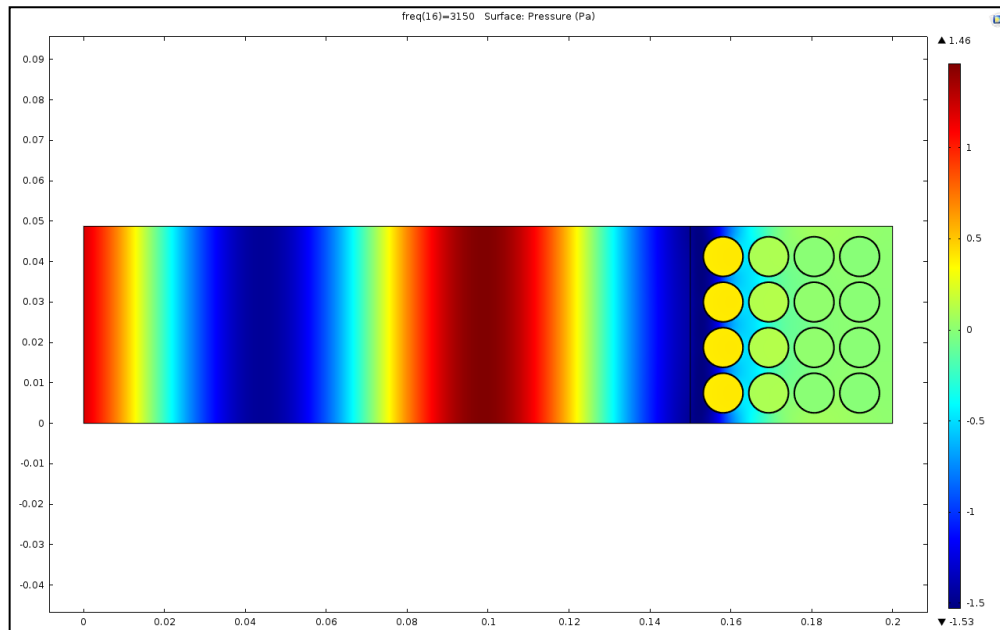


Figure 4.11 Pressure diagram of the air filled pipe embedded absorber for the frequency of 3150 Hz.

The absorption coefficients are shown in Figure 4.12. It is clearly seen that with 3mm, 2 mm, 1 mm and 0.2 mm thicknesses, decreasing the thickness results in higher absorption with 0.2 mm (the thinnest) has shown the best performance, especially in lower frequencies between 100 Hz – 400 Hz.

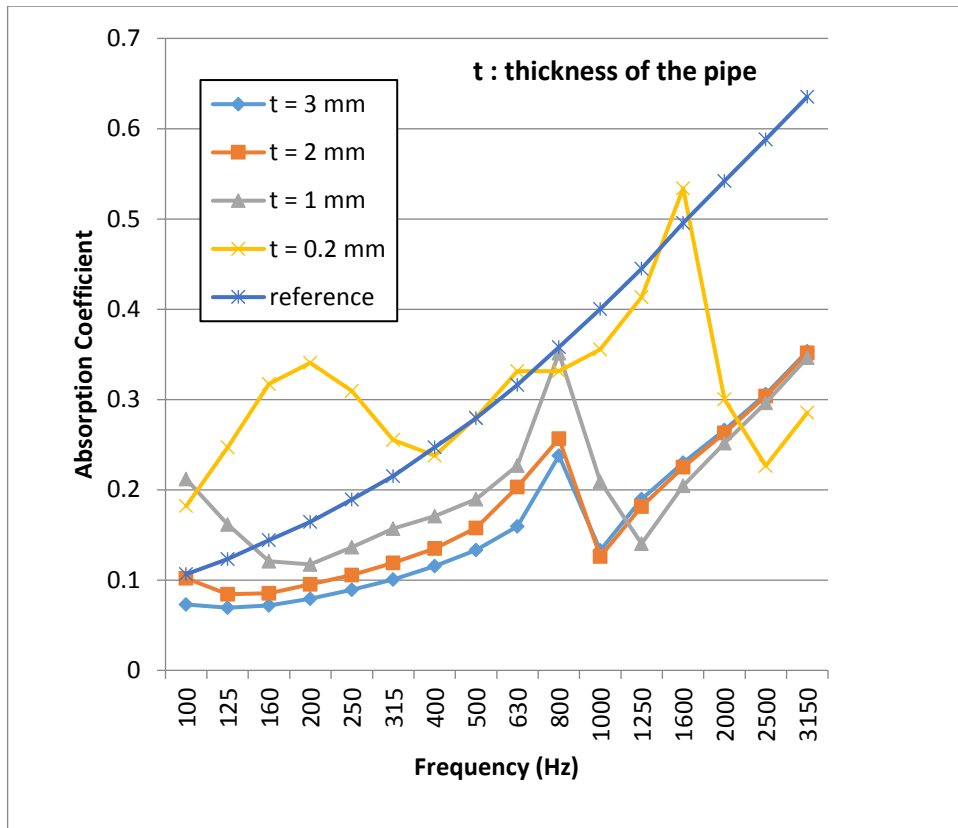


Figure 4.12 Absorption coefficients for the air filled inclusions with the outer diameter of 1 cm with different thickness values.

4.5.1. Applying different outer diameters

In the previous model, it is seen that the most efficient thickness value of the pipe was 0.2mm, the thinnest one. This model contains the same thickness values with different outer diameters, to see the effect to the absorbing characteristics. Pipe structures are shown below (Figure 4.13).

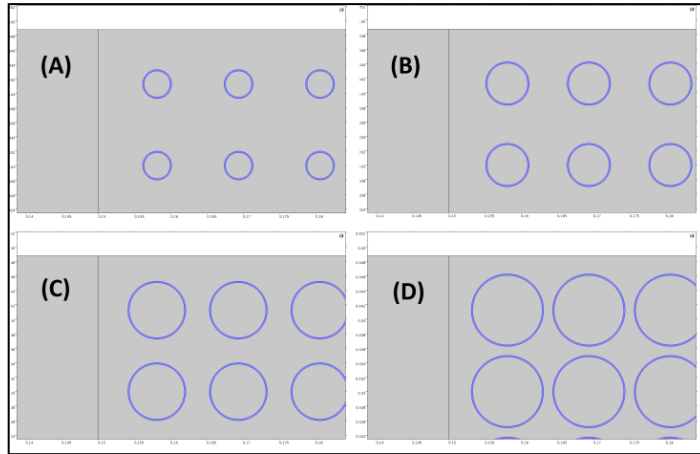


Figure 4.13 Applied outer radiuses, (A) 2mm, (B) 3mm, (C) 4mm, (D) 5mm.

The results showed that the most efficient one is still the one with the largest outer diameter, 1 cm. Corresponding absorption coefficients are shown below (Figure 4.14).

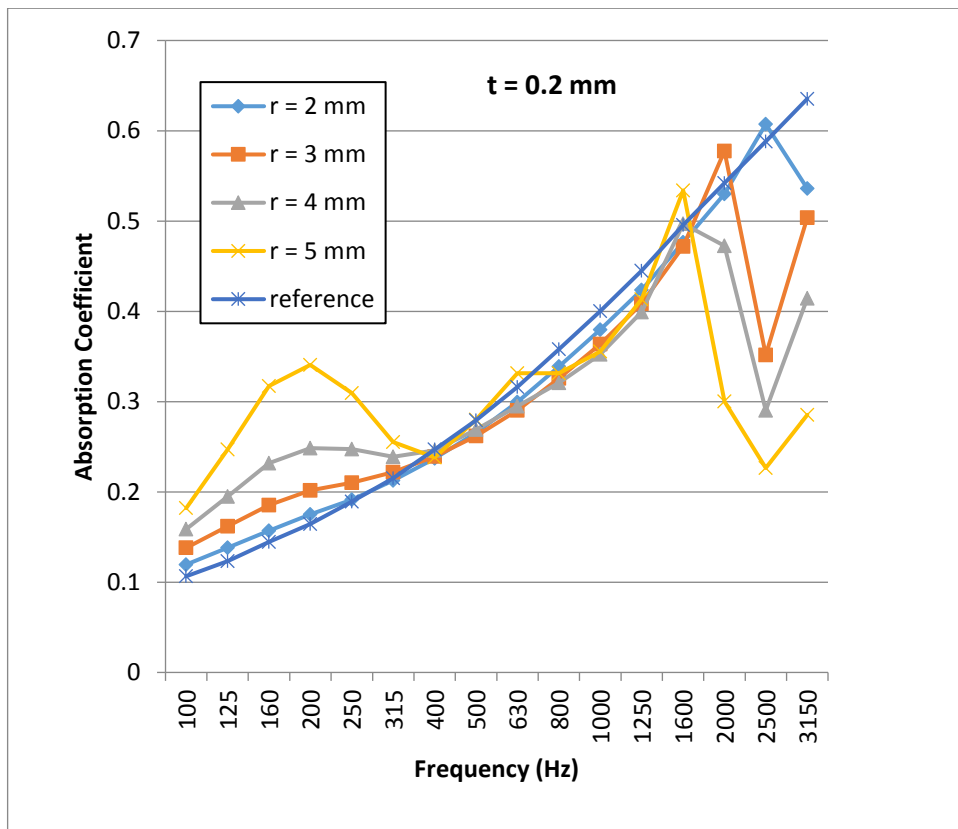


Figure 4.14 Absorption coefficients for different outer diameters, with constant thicknesses, $t = 0.2$ mm.

4.5.2. Applying different materials

It was seen that the best results for the low frequency range in terms of absorption properties is obtained in the absorber which has the thinnest shells covering the cavity and the ones with the largest diameter - Thus same geometric alterations are applied with other pipe materials to see if there might be an improvement with results shown below (Figure 4.15).

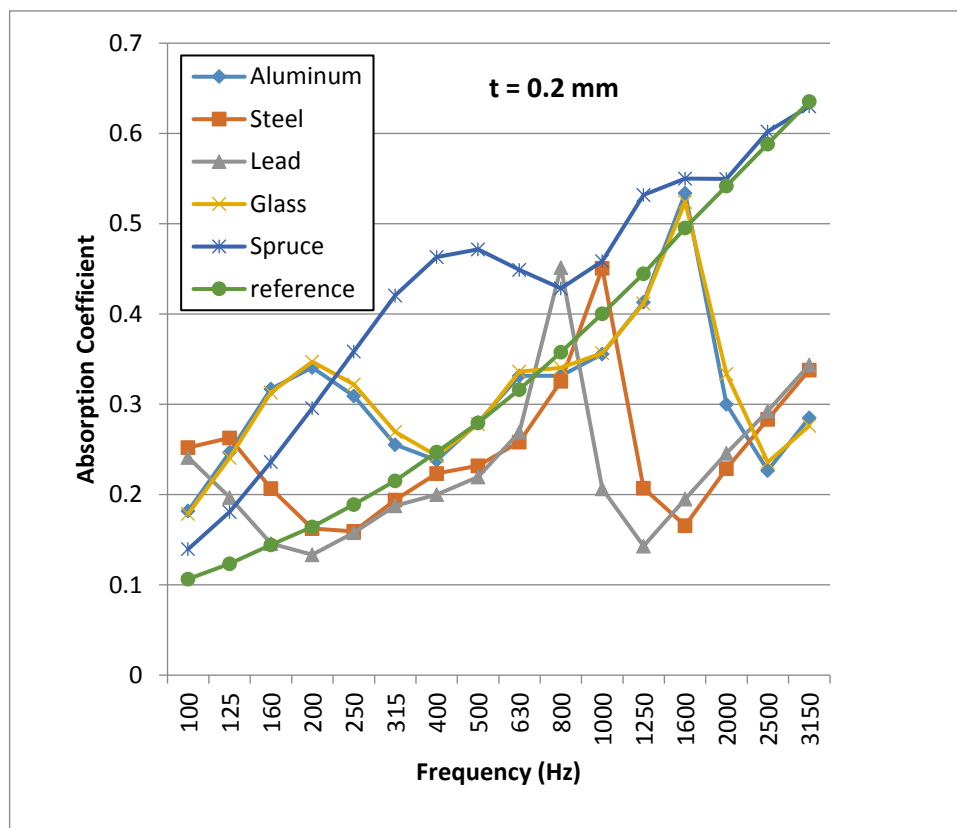


Figure 4.15 Absorption coefficients of the structures with different inclusion materials.

It is clearly seen that the spruce material provides better absorption between 250 Hz - 1000 Hz frequency band, but in the lower frequencies less than 250 Hz, aluminum and glass works much better.

4.5.3. Applying different airflow resistivity values

For improving the effectiveness of the absorber one step further, in the low frequency band, different airflow resistivity values are applied to the same model in the previous section. The results showed that changing the airflow resistivity made a big difference at the absorption properties under 2000 Hz. Especially spruce provide good absorption properties between 250 Hz – 1000 Hz band when compared to the other materials. The absorption coefficients are shown below (Figure 4.16).

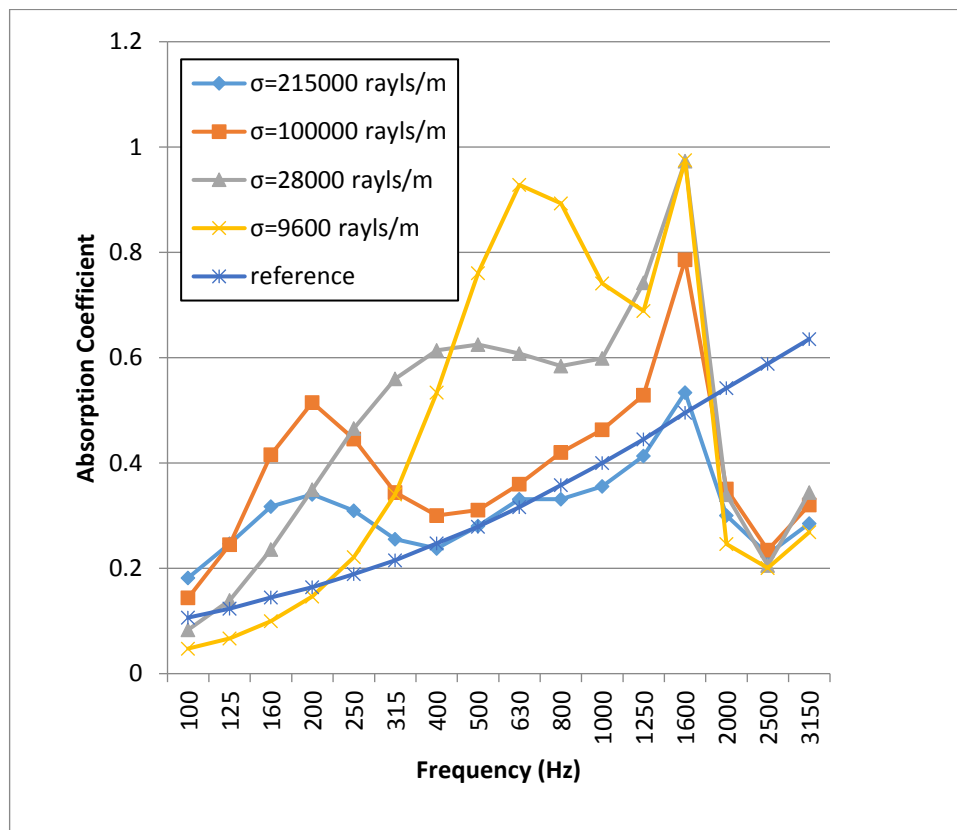


Figure 4.16 Absorption coefficients for different airflow resistivity values.

Up to this part the results of cylindrical additions with various geometric and physical properties have been presented. Square cross-section elements are also investigated instead of cylinder ones, also with and three different wall thicknesses.

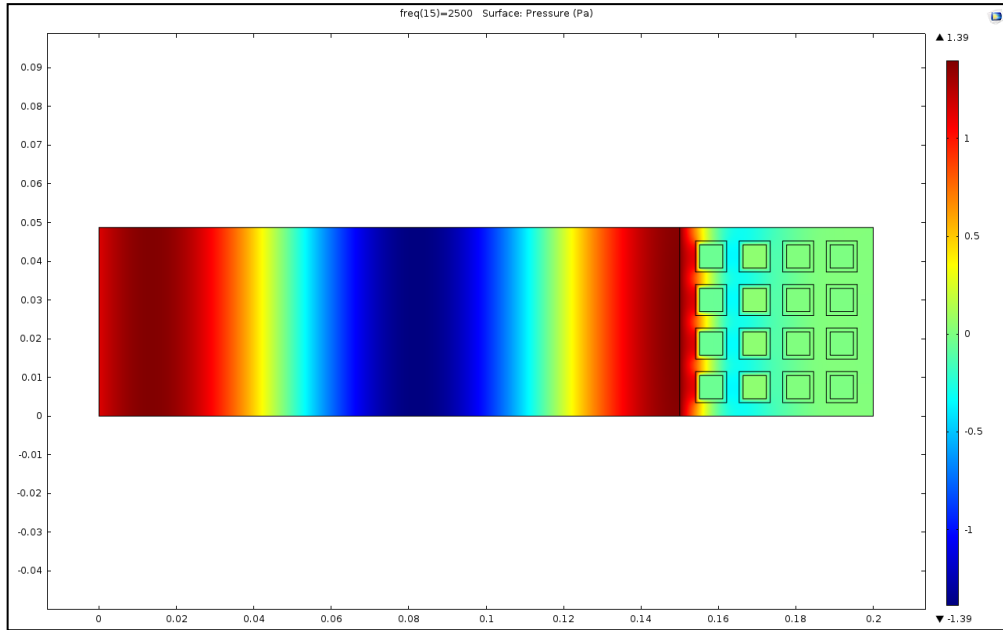


Figure 4.17 Pressure diagram of the square cross-section elements ($t = 2\text{mm}$) including absorber.

The inner parts of the blocks are defined as air, just because it is understood from the previous sections - that foam filling does not make absorber more effective. Pressure diagram of the model and the absorption coefficients are shown in the Figure 4.17 and 18 respectively.

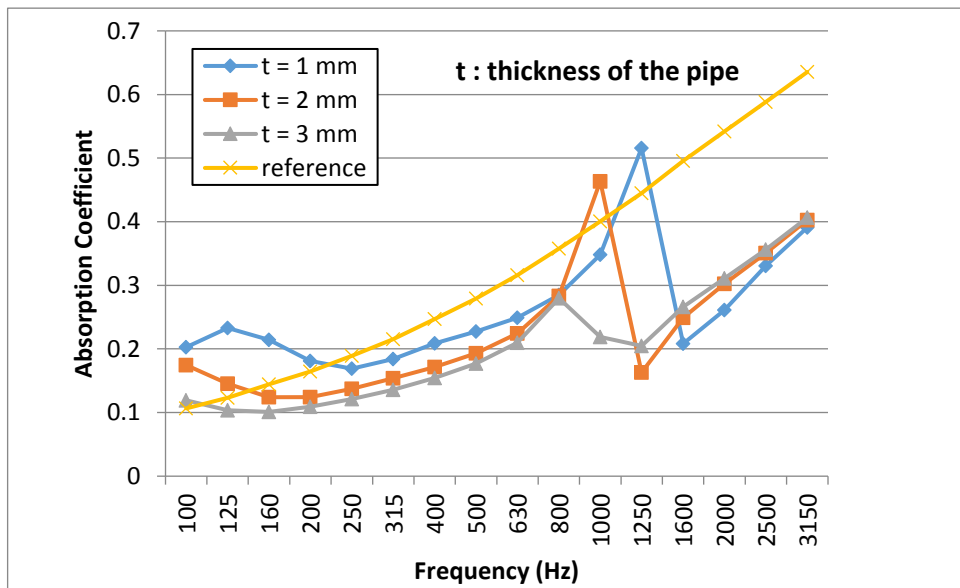


Figure 4.18 Obtained absorption coefficients for the square cross-section blocks.

It is seen that smaller thickness value corresponds to a better absorption properties and absorption coefficients over 0.2, less than 200 Hz is quite high when compared to the foam only.

4.6. Applying Inter-connected Inclusions

It is known that inter-connection in the pores improve the absorption properties of a porous absorber as it was mentioned in the second chapter. In addition to this effect, the inter-connections lead to larger cavities, which have lower resonance frequencies leading to more effective low frequency absorption. In this part the result of inter-connection between resonant elements are demonstrated. These inter-connections are analyzed under 3 cases including, transverse, longitudinal and combined inter-connections.

4.6.1. Transverse inter-connections

Shape and pressure diagrams of the transverse inter-connected elements included in absorber and the obtained absorption coefficients are given in Figure 4.19 and 20 respectively.

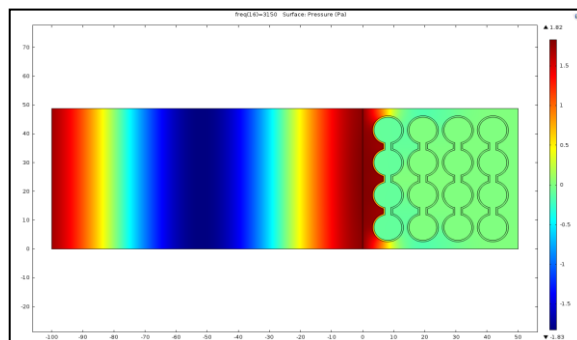


Figure 4.19 Pressure diagram of the transverse inter-connected inclusions added absorber

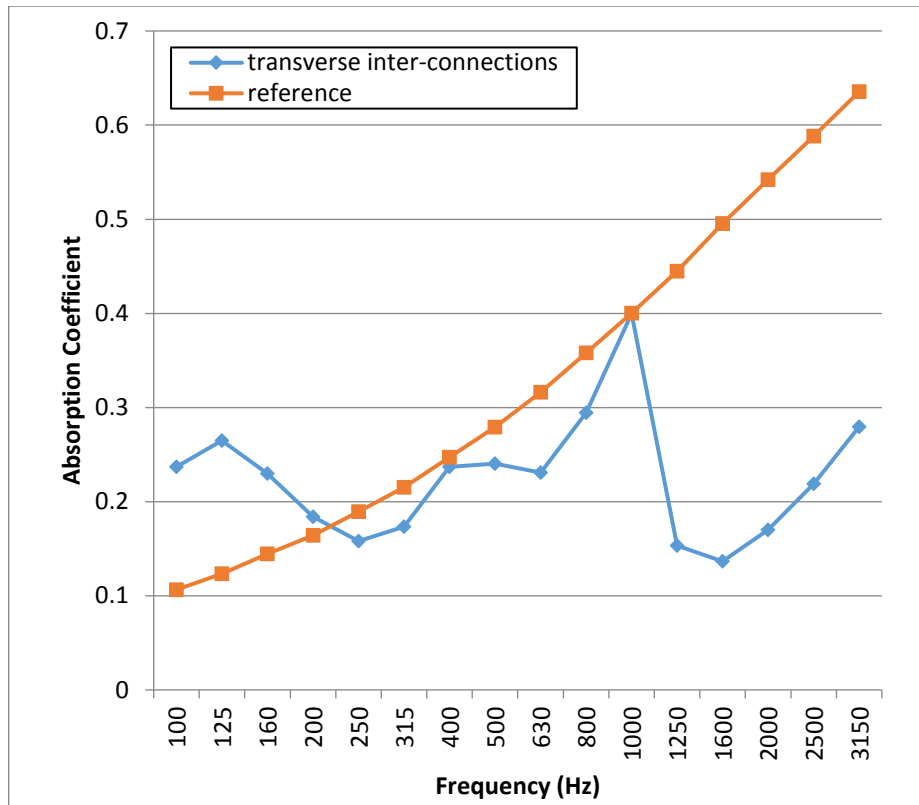


Figure 4.20 The obtained absorption coefficients for the transverse inter-connections including elements added structure

As it is expected, when those inter-connections are transverse, they cause too much reflection and result with poor absorption characteristics.

4.6.2. Longitudinal inter-connections

Pressure diagrams of the transverse inter-connected elements and the corresponding absorption coefficients of the absorber is given in Figure 4.21 and 22 respectively.

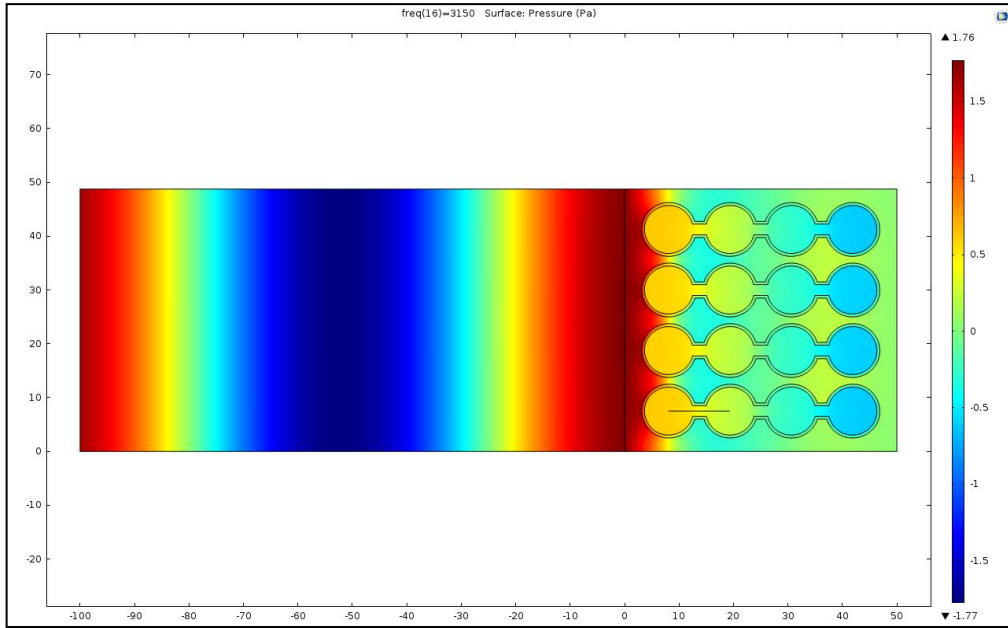


Figure 4.21 Pressure diagram of the longitudinally interconnected inclusions added absorber

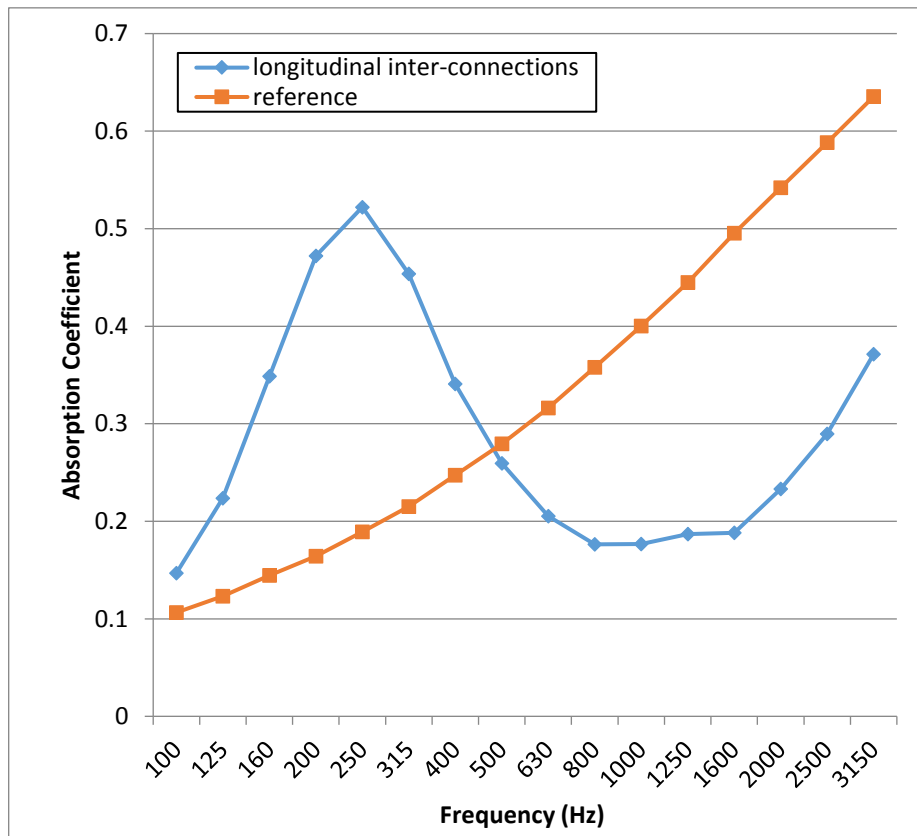


Figure 4.22 Absorption coefficients of longitudinally inter-connected inclusions added absorber

4.6.3. Transverse and longitudinal interconnections

In this part, these longitudinal and transverse inter-connections are combined to see if the performance gets better. Corresponding pressure diagram for 3150 Hz and absorption coefficients are shown in Figure 4.23 and 24 respectively.

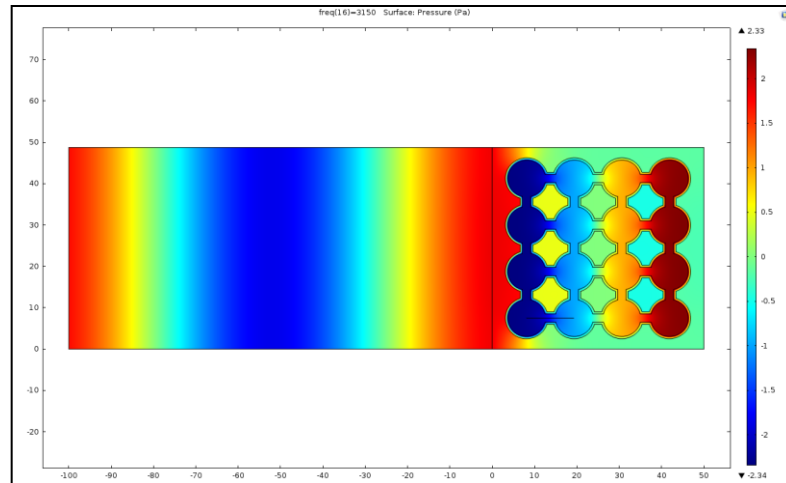


Figure 4.23 Corresponding pressure diagram for 3150 Hz

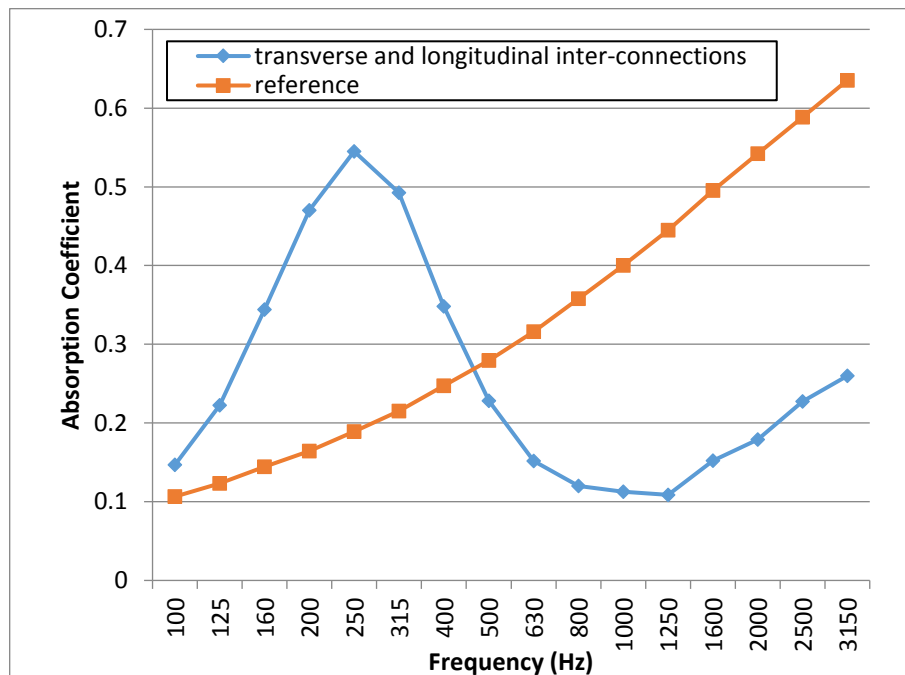


Figure 4.24 The absorption coefficients of the longitudinal inter-connections added elements including absorber

Except the drop in the high frequency performance, in the lower frequencies above 500 Hz, results are quite close to the longitudinal inter-connected elements including absorber. All the results corresponding to this section are shown in Figure 4.25.

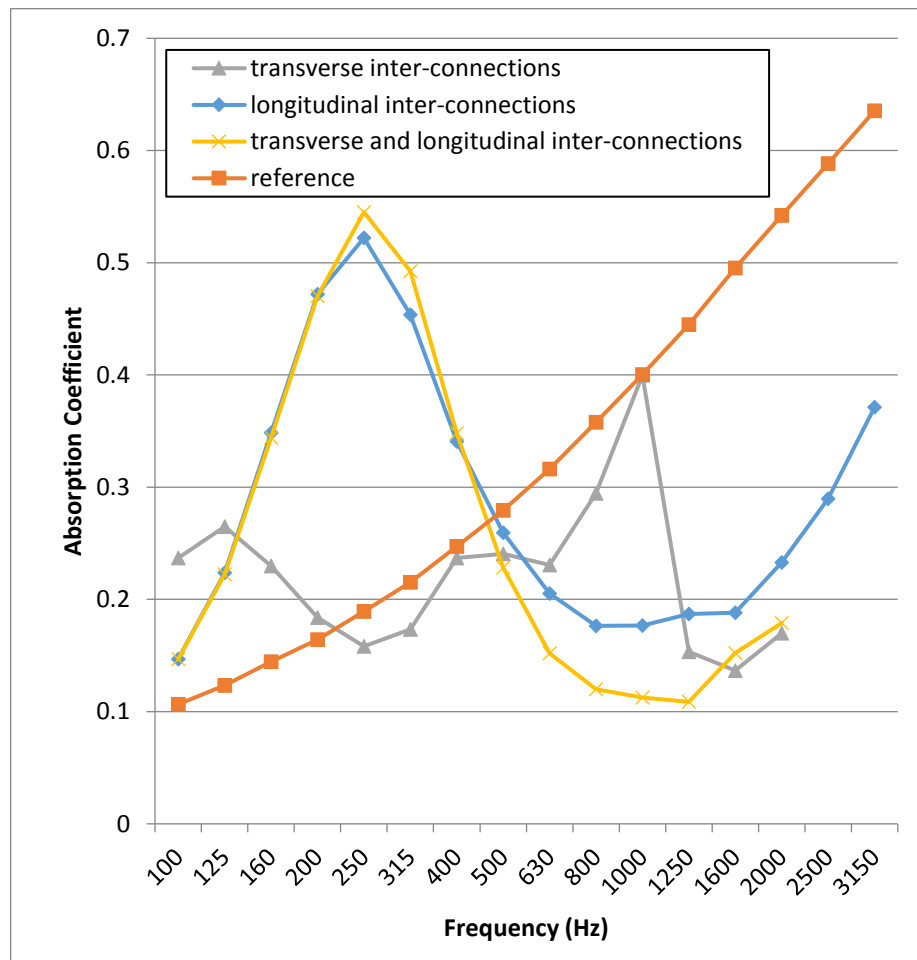


Figure 4.25 Comparison of different inter-connection types

4.7. Longitudinal Air Channels

In the previous sections, it is understood that using longitudinal inter-connections between locally resonant elements is effective in increasing low frequency performance. But when manufacturability is concern, manufacturing such elements with

complex geometry might be problematic. In this section, the geometry is simplified and two different thicknesses are applied.

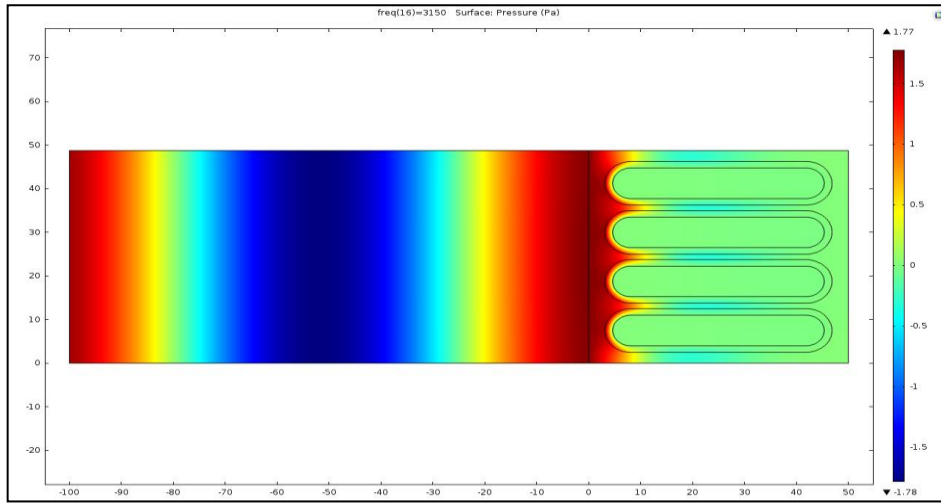


Figure 4.26 The pressure diagram of the generated structure with the thickness value of 1.5 mm in 3150 Hz.

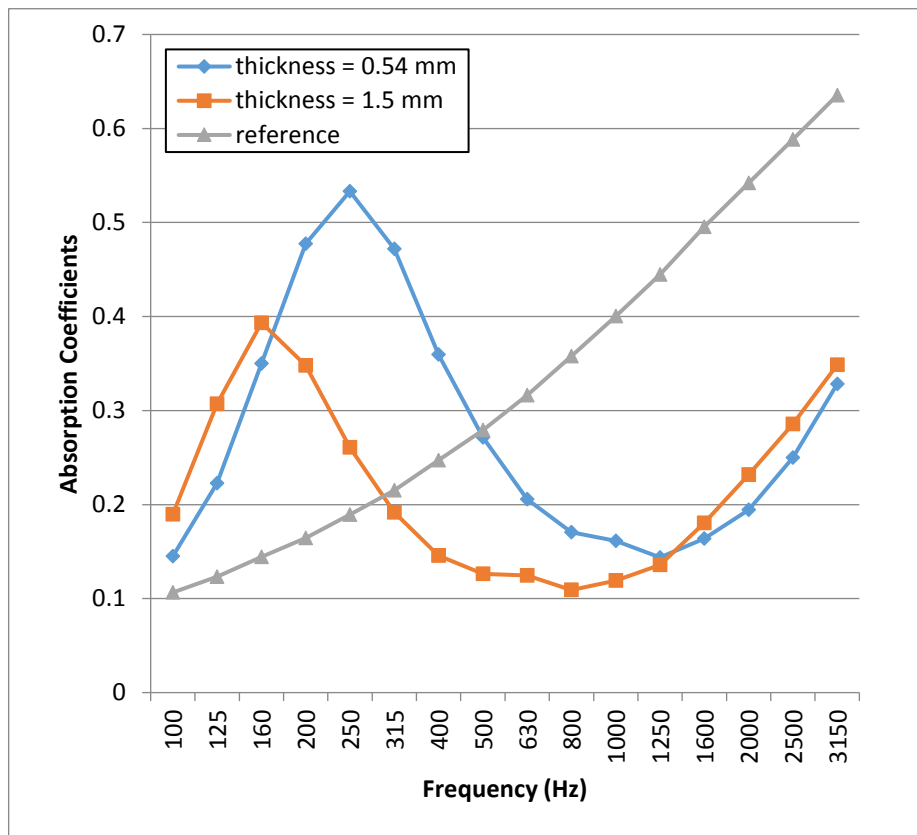


Figure 4.27 The absorption coefficients with different channel thicknesses

The pressure diagram of the generated structure is shown in Figure 4.25. These air channels are demonstrated with two different thickness values, 1.5 mm and 0.54 mm. The absorption coefficients of both models are shown in Figure 4.26. As seen from the figure, the results obtained are close to the longitudinal inter-connected cylinders including structure when the same thickness values are applied (Figure 4.21 and 26). It is understood that the thicker material usage results with worse low frequency performance, but in the frequency ranges higher than 1250 Hz, both channel thickness values result close.

CHAPTER 5

CONCLUSIONS

5.1. Summary and Conclusions

In this study, absorption characteristics of a porous absorber with the addition of mainly cylindrical inclusions were investigated. The inclusions are analyzed with different physical and geometric properties, and material combinations using finite element analysis. First of all, the absorption characteristics of a foam-only absorber is investigated as a basis. The analysis is done using 1/3 octave band frequencies in the range of 100- 3150 Hz. As expected, for the porous material employed, the absorption coefficient increases with increasing frequency in the investigated range, which typically plateaus at higher frequencies. However in the low frequency range, absorption coefficients are very low, ~0.1 at 100 Hz. In order to increase the low frequency performance, a study is performed systematically, analyzing possible alternatives. Adding holes to the porous media was investigated at the first stage. It was observed that an increase in the hole diameter results in increasing absorption coefficients up to 1 cm diameter, however this increment get significant only in frequencies over 400 Hz. Secondly, foam filled cylindrical blocks covered by a thin solid shell with different thickness values are added. Although by using different materials for the blocks, when the blocks are filled with foam, this affected the absorber performance in a negative way. But when those pipes are filled with air, absorption coefficient over 0.3 under 400 Hz frequency band is observed with the smallest thickness value tested. It is shown that using the thinnest shells with the largest air volumes in the porous medium possible, makes a significant improvement in the low frequency absorption. Following the well performing geometry, different inclusion materials: steel, lead, glass and spruce have tested. Glass and aluminum showed similar performance expectedly with their close characteristic impedance values, showing best performance under 250 Hz. But at the frequencies above 315 Hz, spruce has shown the

best performance with absorption coefficient values over 0.4. Up to this step, foam type was taken as default, which has an air flow resistivity of 215000 Rayls/m. Thus, different foam types are tested, to see the effect of the airflow resistivity on the absorption characteristics. And it is shown that lower air flow resistivity values gave the best results for both low and middle frequency values. The results showed that as crucial choosing the right material with the right thickness values is, it is also very important to choose the right foam type to achieve desired sound absorption properties for the related frequency ranges.

Furthermore, interconnections between elements were also investigated. When the inter-connections are applied to the embedded elements, it is seen that low frequency performance below 400 Hz increased significantly and reaching up to absorption coefficient value of 5.2, with a reduction in higher frequency performance. The effect of the orientation of the inter-connections is also investigated. Inter-connections in the direction of the incoming the sound wave performed better than inter-connections in transverse direction. As the final case, the geometry is simplified, to make the design more manufacturable. Longitudinal air channels with different thickness values are tested and their performance has shown to be quite similar to the performance of inter-connected inclusions.

And in this study, it is presented that; it is possible to increase the low frequency performance of foam based porous absorbers by embedding rightly chosen locally resonant inclusions. Since it is known that these acoustic meta-structures can be designed accordingly, they can be optimized for both low and high frequencies at the same time.

5.2. Future Work

This study suggests a solution to the low frequency sound absorption problem, at which the traditional absorbers usually fail. In addition to the provided good performance in low frequencies, in the higher frequencies it remained inefficient. In the future studies, focusing on high frequency sound absorption without losing the low

frequency performance will give a chance to design wideband absorbers. Also, another planned future work is utilizing natural materials such as wood, stone, marble, mud, plants, and bushes to provide more environmentally-friendly solutions to large-scale noise control problems. Also, in addition to the normal incidence considerations, the absorbers should be designed for random incidence for effective sound absorption. Acoustic meta-materials are known to be efficient in random incidence, as much as they are in normal incidence, which makes them a good candidate for the proposed solution.

REFERENCES

- [1] G.-F. C. Peisheng Liu, *Porous Materials: Processing and Applications*. 2014.
- [2] T. J. Cox and P. D'Antonio, *Acoustic Absorbers and Diffusers: Theory, Design and Application*, vol. 25, no. 9. 2009.
- [3] P. Jones and N. Kessissoglou, "Measurement and prediction of the acoustic performance of poroelastic foam filled mufflers for sleep apnoea devices," no. August, pp. 1–6, 2010.
- [4] K. V Horoshenkov and M. J. Swift, "The acoustic properties of granular materials with pore size distribution close to log-normal.," *J. Acoust. Soc. Am.*, vol. 110, no. April, pp. 2371–2378, 2001.
- [5] J. Pfretzschner, "Rubber crumb as granular absorptive acoustic material," in *Proc. Forum Acusticum, Sevilla, 2002*, pp. MAT–01–005–IP.
- [6] D. A. Bies and C. H. Hansen, *Engineering noise control: theory and practice*, vol. 3. 2003.
- [7] L. L. Beranek and I. L. Vér, *Noise and Vibration Control Engineering*. 1992.
- [8] M. E. Delany and E. N. Bazley, "Acoustical properties of fibrous absorbent materials," *Appl. Acoust.*, vol. 3, no. 2, pp. 105–116, 1970.
- [9] C. Lagarrigue, J. P. Groby, V. Tournat, O. Dazel, and O. Umnova, "Absorption of sound by porous layers with embedded periodic arrays of resonant inclusions," *J. Acoust. Soc. Am.*, vol. 134, no. 6, pp. 4670–4680, 2013.
- [10] O. Doutres, N. Atalla, and H. Osman, "Transfer matrix modeling and experimental validation of cellular porous material with resonant inclusions," *J. Acoust. Soc. Am.*, vol. 137, no. 6, pp. 3502–3513, 2015.
- [11] D.-Y. Maa, "Microperforated-panel wideband absorbers," *Noise Control Eng. J.*, vol. 29, no. 3, pp. 77–84, 1987.
- [12] "http://www.yamahaproaudio.com/global/en/training_support/selftraining/audio_quality/chapter4/01_ear_anatomy/." .
- [13] "<http://image.slidesharecdn.com/11-141120093650-conversion-gate02/95/frequencyplacettransformation-20-638.jpg?cb=1423404234>."
- [14] "<http://global.britannica.com/science/phonon>." .

- [15] S. Kim and S. Lee, “Air transparent soundproof window,” vol. 117123, p. 4, 2013.
- [16] M. Farhat, S. Enoch, S. Guenneau, and A. B. Movchan, “Broadband cylindrical acoustic cloak for linear surface waves in a fluid,” *Phys. Rev. Lett.*, vol. 101, no. 13, 2008.
- [17] L. Zigoneanu, B.-I. Popa, and S. a Cummer, “Three-dimensional broadband omnidirectional acoustic ground cloak,” *Nat. Mater.*, vol. 13, no. March, pp. 1–4, 2014.
- [18] J. S. Bolton, N.-M. Shiau, and Y. J. Kang, “Sound transmission through multi-panel structures lined with elastic porous materials,” *J. Sound Vib.*, vol. 191, no. 3, pp. 317–347, 1996.
- [19] “http://www.naturalnews.com/043383_metamaterials_earthquake-resistant_buildings_invisibility.html.”
- [20] M. M. Sigalas and E. N. Economou, “Elastic waves in plates with periodically placed inclusions,” *J. Appl. Phys.*, vol. 75, no. 6, pp. 2845–2850, 1994.
- [21] R. Martínez-Sala, J. Sancho, J. V. Sánchez, V. Gómez, J. Llinares, and F. Meseguer, “Sound attenuation by sculpture,” *Nature*, vol. 378, no. 6554. pp. 241–241, 1995.
- [22] Z. Liu, “Locally Resonant Sonic Materials,” *Science (80-.)*, vol. 289, no. 5485, pp. 1734–1736, 2000.
- [23] A. O. Krushynska, V. G. Kouznetsova, and M. G. D. Geers, “Towards optimal design of locally resonant acoustic metamaterials,” *J. Mech. Phys. Solids*, vol. 71, no. 1, pp. 179–196, 2014.
- [24] Y. L. Tsai and T. Chen, “Band gap structure of acoustic wave in hexagonal phononic crystals with polyethylene matrix,” in *Procedia Engineering*, 2014, vol. 79, pp. 612–616.
- [25] X. Hu, C. T. Chan, and J. Zi, “Two-dimensional sonic crystals with Helmholtz resonators,” *Phys. Rev. E - Stat. Nonlinear, Soft Matter Phys.*, vol. 71, no. 5, pp. 1–4, 2005.
- [26] C. Goffaux, J. Sánchez-Dehesa, and P. Lambin, “Comparison of the sound attenuation efficiency of locally resonant materials and elastic band-gap structures,” *Phys. Rev. B - Condens. Matter Mater. Phys.*, vol. 70, no. 18, pp. 1–6, 2004.
- [27] B. Djafari-Rouhani, J. O. Vasseur, A. C. Hladky-Hennion, P. Deymier, F. Duval, B. Dubus, and Y. Pennec, “Absolute band gaps and waveguiding in free standing and supported phononic crystal slabs,” *Photonics Nanostructures - Fundam.*

- Appl.*, vol. 6, no. 1, pp. 32–37, 2008.
- [28] T. T. Wu, Z. G. Huang, T. C. Tsai, and T. C. Wu, “Evidence of complete band gap and resonances in a plate with periodic stubbed surface,” *Appl. Phys. Lett.*, vol. 93, no. 11, pp. 113–115, 2008.
- [29] D. Torrent and V. M. Garc, “Quasi-two-dimensional acoustic metamaterials for sound control in ducts,” pp. 4–6, 2013.
- [30] Daniel Peter Eford, “Band gap formation in acoustically resonant phononic crystals,” Loughborough University, 2010.
- [31] M. Hirsekorn, P. P. Delsanto, A. C. Leung, and P. Matic, “Elastic wave propagation in locally resonant sonic material: Comparison between local interaction simulation approach and modal analysis,” *J. Appl. Phys.*, vol. 99, no. 12, 2006.
- [32] J. G. Hu and W. Xu, “Band structures of phononic crystal composed of lattices with different periodic constants,” *Phys. B Condens. Matter*, vol. 441, pp. 89–93, 2014.
- [33] G. Ma and P. Sheng, “Acoustic metamaterials: From local resonances to broad horizons,” *Sci. Adv.*, vol. 2, no. 2, p. e1501595, 2016.
- [34] S. A. Cummer, J. Christensen, and A. Alù, “Controlling sound with acoustic metamaterials,” *Nat. Rev. Mater.*, vol. 1, no. 3, p. 16001, 2016.
- [35] S. Zhang, C. Xia, and N. Fang, “Broadband acoustic cloak for ultrasound waves,” *Phys. Rev. Lett.*, vol. 106, no. 2, 2011.
- [36] Y. Cheng, F. Yang, J. Y. Xu, and X. J. Liu, “A multilayer structured acoustic cloak with homogeneous isotropic materials,” *Appl. Phys. Lett.*, vol. 92, no. 15, 2008.
- [37] H. Shen, M. P. Païdoussis, J. Wen, D. Yu, L. Cai, and X. Wen, “Acoustic cloak/anti-cloak device with realizable passive/active metamaterials,” *J. Phys. D. Appl. Phys.*, vol. 45, no. 28, p. 285401, 2012.
- [38] V. M. García-Chocano, L. Sanchis, A. Díaz-Rubio, J. Martínez-Pastor, F. Cervera, R. Llopis-Pontiveros, and J. Sánchez-Dehesa, “Acoustic cloak for airborne sound by inverse design,” *Appl. Phys. Lett.*, vol. 99, no. 7, 2011.
- [39] T. Miyashita, “Sonic crystals and sonic wave-guides,” *Meas. Sci. Technol.*, vol. 16, no. 5, pp. R47–R63, 2005.
- [40] S. Yao, P. Li, X. Zhou, and G. Hu, “Sound reduction by metamaterial-based acoustic enclosure,” *AIP Adv.*, vol. 4, no. 12, 2014.

- [41] S. Varanasi, J. S. Bolton, T. H. Siegmund, and R. J. Cipra, “The low frequency performance of metamaterial barriers based on cellular structures,” *Appl. Acoust.*, vol. 74, no. 4, pp. 485–495, 2013.
- [42] H. Meng, J. Wen, H. Zhao, and X. Wen, “Optimization of locally resonant acoustic metamaterials on underwater sound absorption characteristics,” *J. Sound Vib.*, vol. 331, no. 20, pp. 4406–4416, 2012.
- [43] L. M. Hao, C. L. Ding, and X. P. Zhao, “Tunable acoustic metamaterial with negative modulus,” *Appl. Phys. A Mater. Sci. Process.*, vol. 106, no. 4, pp. 807–811, 2012.
- [44] M. D. Guild, V. M. García-Chocano, W. Kan, and J. Sánchez-Dehesa, “Acoustic metamaterial absorbers based on multilayered sonic crystals,” *J. Appl. Phys.*, vol. 117, no. 11, 2015.
- [45] J. M. P. Ant?nio, A. Tadeu, and L. Godinho, “Analytical evaluation of the acoustic insulation provided by double infinite walls,” *J. Sound Vib.*, vol. 263, no. 1, pp. 113–129, 2003.
- [46] S. E. Makris, C. L. Dym, and J. M. Smit, “Transmission loss optimization in acoustic sandwich panels,” *J. Acoust. Soc. Am.*, vol. 79, no. 6, p. 1833, 1986.
- [47] W. . Tang, H. Zheng, and C. . Ng, “Low frequency sound transmission through close-fitting finite sandwich panels,” *Appl. Acoust.*, vol. 55, no. 1, pp. 13–30, Sep. 1998.
- [48] Z. Yang, H. M. Dai, N. H. Chan, G. C. Ma, and P. Sheng, “Acoustic metamaterial panels for sound attenuation in the 50 – 1000 Hz regime,” pp. 3–5, 2010.
- [49] D. Oliva and V. Hongisto, “Sound absorption of porous materials – Accuracy of prediction methods,” *Appl. Acoust.*, vol. 74, no. 12, pp. 1473–1479, 2013.
- [50] P. W. Jones, “PREDICTION OF THE ACOUSTIC PERFORMANCE OF SMALL POROELASTIC FOAM FILLED MUFFLERS : A CASE STUDY,” vol. 38, no. 2, pp. 69–75, 2010.

APPENDIX A

MATLAB CODE FOR EMPIRICAL SOLUTION OF POROUS LAYER

```
%METHOD 7 - THEORETICAL APPROACH
f=[100;125;160;200;250;315;400;500;630;800;1000;1250;1600;2000;2500;31
50]
c=344
ro=1.204
a=215000
d=0.018
Z0=ro*c

%DELANY&BAZLEY COEFFICIENTS
c1=0.05710
c2=-0.75400
c3=0.08700
c4=-0.73200
c5=0.18900
c6=-0.59500
c7=0.09780
c8=-0.70000

%X CALCULATION
for k=1:16
X(k,1)=((ro*f(k,1))/a)
end
X

%Z1 CALCULATION
for k=1:16
Z1(k,1)=Z0*(1+(c1*(X(k,1)^c2))-1i*(c3*(X(k,1)^c4)))
end
Z1

%w calculation
for k=1:16
w(k,1)=(2*pi()*f(k,1))
end
w

%r CALCULATION (PROPAGATION CONSTANT)
for k=1:16
r(k,1)=(w(k,1)/c)*((c5*(X(k,1)^c6))+1i*((1+(c7*(X(k,1)^c8))))))
end
r

%ZS1 CALCULATION
```

```

for k=1:16
ZS1(k,1)=Z1(k,1)*(coth(r(k,1)*d))
end
ZS1

%RE CALCULATION(REFLECTION FACTOR)
for k=1:16
RE(k,1)=(ZS1(k,1)-Z0)/(ZS1(k,1)+Z0)
end
RE

%GAMA CALCULATION(ABSORPTION COEFFICIENT)
for k=1:16
GAMA(k,1)=1-(abs((RE(k,1))^2))
end
GAMA

plot(f,GAMA)

```

APPENDIX B

MATLAB CODE FOR ABSORPTION COEFFICIENTS

```
%COMPLEX RATIO CALCULATION
for k=1:16
complexratio(k,1)=mic2(k,1)/mic1(k,1);
end
complexratio

c=344;
ro=1.204;
lx=0.018;
dx=0.018;

%ZS1 CALCULATION
for k=1:16
ZS1(k,1)=1i*ro*c*(((complexratio(k,1)*sin((2*pi()*frequency(k,1)/c)*(
lx+dx))))-
sin((2*pi()*frequency(k,1)/c)*(lx)))/(cos((2*pi()*frequency(k,1)/c)*lx
)-(complexratio(k,1)*cos((2*pi()*frequency(k,1)/c)*(lx+dx))));
end
ZS1

%R CALCULATION
for k=1:16
r(k,1)=(ZS1(k,1)-(c*ro))/(ZS1(k,1)+(c*ro))
end
r

%ALFA (ABSORPTION COEFFICIENT) CALCULATION
for k=1:16
alfa(k,1)=(1-(abs(r(k,1)))^2)
end
alfa

plot(frequency, alfa)
```